Chapter 9
Models for Influenza

9.1 Introduction to Influenza Models

Influenza causes more morbidity and more mortality than all other respiratory diseases together. There are annual seasonal epidemics that cause about 500, 000 deaths worldwide each year. During the twentieth century there were three influenza pandemics. The World Health Organization estimates that there were 40, 000, 000–50, 000, 000 deaths worldwide in the 1918 pandemic, 2, 000, 000 deaths worldwide in the 1957 pandemic, and 1, 000, 000 deaths worldwide in the 1968 pandemic. There has been concern since 2005 that the H5N1 strain of avian influenza could develop into a strain that can be transmitted readily from human to human and develop into another pandemic, together with a widely held belief that even if this does not occur there is likely to be an influenza pandemic in the near future. More recently, the H1N1 strain of influenza did develop into a pandemic in 2009, but fortunately its case mortality rate was low and this pandemic turned out to be much less serious than had been feared. There were 18,500 confirmed deaths, but the actual number of deaths caused by the H1N1 influenza may have been as many as 200,000. This history has aroused considerable interest in modeling both the spread of influenza and comparison of the results of possible management strategies.

Vaccines are available for annual seasonal epidemics. Influenza strains mutate rapidly, and each year a judgment is made of which strains of influenza are most likely to invade. A vaccine is distributed that protects against the three strains considered most dangerous. However, if a strain radically different from previously known strains arrives, vaccine provides little or no protection and there is danger of a pandemic. As it would take at least 6 months to develop a vaccine to protect against such a new strain, it would not be possible to have a vaccine ready to protect against the initial onslaught of a new pandemic strain. Attempts are underway to try to develop a more universal vaccine.

F. Brauer et al., *Mathematical Models in Epidemiology*, Texts in Applied Mathematics 69, https://doi.org/10.1007/978-1-4939-9828-9_9

Antiviral drugs are available to treat pandemic influenza, and they may have some preventive benefits as well, but such benefits are present only while antiviral treatment is continued.

Various kinds of models have been used to describe influenza outbreaks. Many public health policy decisions on coping with a possible influenza pandemic are based on construction of a contact network for a population and analysis of disease spread through this network. This analysis consists of multiple stochastic simulations requiring a substantial amount of computer time. In advance of an epidemic it is not possible to know its severity, and it would be necessary to make estimates for a range of reproduction numbers. Also, model parameters for the H1N1 influenza pandemic of 2009, especially the susceptibility to infection for different age groups, were significantly different from those for seasonal epidemics. In advance of an anticipated pandemic it may be more appropriate to use simpler models until enough data are acquired to facilitate parameter estimation. Early estimation of model parameters is extremely important for coping with a serious epidemic, and one of the outcomes of the H1N1 influenza pandemic of 2009 was development of new methods, mainly based on network models, to achieve this.

Our approach is to begin with simple models and to add more structure later as more information is obtained. When an epidemic does begin, plans for management strategies need to be very detailed, and use of the simple models we describe here should be restricted to advance planning and broad understanding.

We begin this chapter by developing a simple compartmental influenza transmission model and then augmenting it to include both pre-epidemic vaccination and treatment during an epidemic. We will also describe some ways in which the model can be modified to be more realistic, though more complicated. The development follows the treatment in [6, 7]. We will describe the models and the results of their analyses, but omit proofs in order to focus attention on the applications of the models. Many of the results may be found in earlier chapters.

9.2 A Basic Influenza Model

Since influenza epidemics usually come and go in a time period of several months, we do not include demographic effects (births and natural deaths) in our model. Our starting point is the simple SIR model. Two aspects of influenza that are easily added are that there is an incubation period between infection and the appearance of symptoms, and that a significant fraction of people who are infected never develop symptoms but go through an asymptomatic period, during which they have some infectivity, and then recover and go to the removed compartment [35]. Thus a model should contain the compartments S (susceptible), L (latent), I (infective), A (asymptomatic), and R (removed). Specifically, we make the following assumptions:

1. There is a small number I_0 of initial infectives in a population of constant total size N.

2. The number of contacts in unit time per individual is a constant multiple β of total population size N.
3. Latent members (L) are not infective.
4. A fraction p of latent members proceed to the infective compartment at rate κ, while the remainder goes directly to an asymptomatic infective compartment (A), also at rate κ.
5. There are no disease deaths; infectives (I) recover and leave the infective compartment at rate α, and go to the removed compartment (R).
6. Asymptomatics have infectivity reduced by a factor δ, and go to the removed compartment at rate η.

These assumptions lead to the model

$$\begin{aligned} S' &= -S\beta(I + \delta A) \\ L' &= S\beta(I + \delta A) - \kappa L \\ I' &= p\kappa L - \alpha I \\ A' &= (1 - p)\kappa L - \eta A \\ R' &= \alpha I + \eta A \end{aligned} \tag{9.1}$$

with initial conditions

$$S(0) = S_0, \quad L(0) = 0, \quad I(0) = I_0, \quad A(0) = 0, \quad R(0) = 0, \quad N = S_0 + I_0.$$

In analyzing this model we may remove one variable since $N = S + L + I + A + R$ is constant. It is usually convenient to remove the variable R. It is possible to show that the model (9.1) is properly posed in the sense that all variables remain non-negative for $0 \leq t < \infty$. A flow diagram for the model (9.1) is shown in Fig. 9.1. The model (9.1) is the simplest possible description for influenza having the property that there are asymptomatic infections. The question that should be in the back of our minds is whether it is a sufficiently accurate description for its predictions to be useful.

The model (9.1), like the other models that we will introduce later, consists of a system of ordinary differential equations. The number of susceptibles in the population tends to a limit S_∞ as $t \to \infty$ and the final size relation may be used to find this limit without the need to solve the system of differential equations. It is more realistic to assume saturation of contacts and that β is a function of the total population size N. In general, the final size relation is an inequality. If there are no disease deaths, N is constant and β is constant even with saturation of contacts. If the disease death rate is small, it appears that the final size relation is very close to an equality and it is reasonable to assume that β is constant and use the final size relation as an equation to solve for S_∞.

We may use the next generation matrix approach of [48] to calculate the basic reproduction number

$$\mathscr{R}_0 = \beta N \left[\frac{p}{\alpha} + \frac{\delta(1 - p)}{\eta} \right]. \tag{9.2}$$

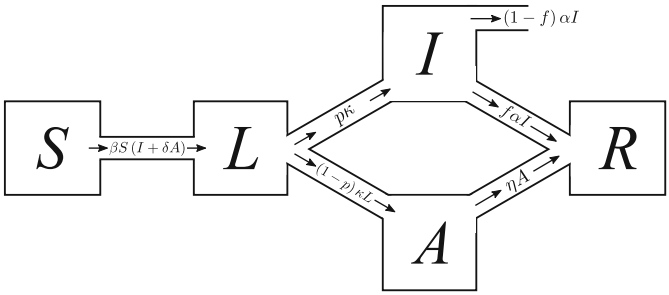

Fig. 9.1 Diagram for the basic influenza model (9.1)

A biological interpretation of this basic reproduction number is that a latent member introduced into a population of N susceptibles becomes infective with probability p, in which case he or she causes $\beta N/\alpha$ infections during an infective period of length $1/\alpha$, or becomes asymptomatic with probability $1-p$, in which case he or she causes $\delta\beta N/\eta$ infections during an asymptomatic period of length $1/\eta$.

The *final size relation* is given by

$$\log \frac{S_0}{S_\infty} = \mathscr{R}_0 \left[1 - \frac{S_0}{N}\right]. \tag{9.3}$$

A very general form of the final size relation that is applicable to each of the models in this chapter is derived in Sect. 4.5. The final size relation shows that $S_\infty > 0$. This means that some members of the population are not infected during the epidemic. The size of the epidemic, the number of (clinical) cases of influenza during the epidemic, is

$$I_0 + S_0 - S_\infty = N - S_\infty,$$

and the number of symptomatic cases is

$$I_0 + p(S_0 - S_\infty).$$

If there are disease deaths, with a disease survival rate f and a disease death rate $(1-f)$ among infectives (assuming no disease deaths of asymptomatics), the number of disease deaths is

$$I_0 + (1-f)p(S_0 - S_\infty).$$

While mathematicians view the basic reproduction number as central in studying epidemiological models, epidemiologists may be more concerned with the *attack rate*, as this may be measured directly. For influenza, where there are asymptomatic

cases, there are two attack rates. One is the clinical attack rate, which is the fraction of the population that becomes infected, defined as

$$1 - \frac{S_\infty}{N}.$$

There is also the symptomatic attack rate, defined as the fraction of the population that develops disease symptoms, defined as

$$p\left[1 - \frac{S_\infty}{N}\right].$$

The attack rates and the basic reproduction number are connected through the final size relation (9.3). If we know the parameters of the model we can calculate $\mathscr{R}_0$ from (9.2) and then solve for S_∞ from (9.3).

We apply the model (9.1) using parameters appropriate for the 1957 influenza pandemic as suggested by [35]. The latent period is approximately 1.9 days and the infective period is approximately 4.1 days, so that

$$\kappa = \frac{1}{1.9} = 0.526, \quad \alpha = \eta = \frac{1}{4.1} = 0.244.$$

We also take

$$p = 2/3, \quad \delta = 0.5, \quad f = 0.98.$$

As in [35] we consider a population of 2000 members, of whom 12 are infective initially. In [35] a symptomatic attack rate was assumed for each of the four age groups, and the average symptomatic attack rate for the entire population was 0.326. This implies $S_\infty = 1022$. Then we obtain

$$\mathscr{R}_0 = 1.37$$

from (9.3). Now, we use this in (9.2) to calculate

$$\beta N = 0.402.$$

We will use these data as baseline values to estimate the effect that control measures might have had. The number of clinical cases is 978 (including the initial 12), the number of symptomatic cases is 664, again including the original 12, and the number of disease deaths is approximately 13.

The model (9.1) can be adapted to describe management strategies for both annual seasonal epidemics and pandemics.

9.2.1 Vaccination

To cope with annual seasonal influenza epidemics, there is a program of vaccination before the "flu" season begins. Each year a vaccine is produced aimed at protecting against the three influenza strains considered most dangerous for the coming season. We formulate a model to add vaccination to the model described by (9.1) under the assumption that vaccination reduces susceptibility (the probability of infection if a contact with an infected member of the population is made). In addition, if we assume that vaccinated members who develop infection are less likely to transmit infection, more likely not to develop symptoms, and are likely to recover more rapidly than unvaccinated members.

These assumptions require us to introduce additional compartments into the model to follow treated members of the population through the stages of infection. We use the classes S, L, I, A, R as before and introduce S_T, the class of treated susceptibles, L_T, the class of treated latent members, I_T, the class of treated infectives, and A_T, the class of treated asymptomatics. In addition to the assumptions made in formulating the model (9.1) we also assume

- A fraction γ of the population is vaccinated before a disease outbreak and vaccinated members have susceptibility to infection reduced by a factor σ_S.
- There are decreases σ_I and σ_A, respectively, in infectivity in I_T, and A_T; it is reasonable to assume

$$\sigma_I < 1, \quad \sigma_A < 1.$$

- The rates of departure from L_T, I_T, and A_T are κ_T, α_T, and η_T, respectively. It is reasonable to assume

$$\kappa \leq \kappa_T, \quad \alpha \leq \alpha_T, \quad \eta \leq \eta_T.$$

- The fractions of members recovering from disease when they leave I and I_T are f and f_T, respectively. It is reasonable to assume $f \leq f_T$. In our analysis we will take $f = f_T = 1$ (no disease deaths).
- Vaccination decreases the fraction of latent members who will develop symptoms by a factor τ, with $0 \leq \tau \leq 1$.

For convenience we introduce the notation

$$Q = I + \delta A + \sigma_I I_T + \delta \sigma_A A_T. \tag{9.4}$$

The resulting model is

$$\begin{aligned} S' &= -S\beta Q \\ S_T' &= -\sigma_S S_T \beta Q \\ L' &= S\beta Q - \kappa L \end{aligned}$$

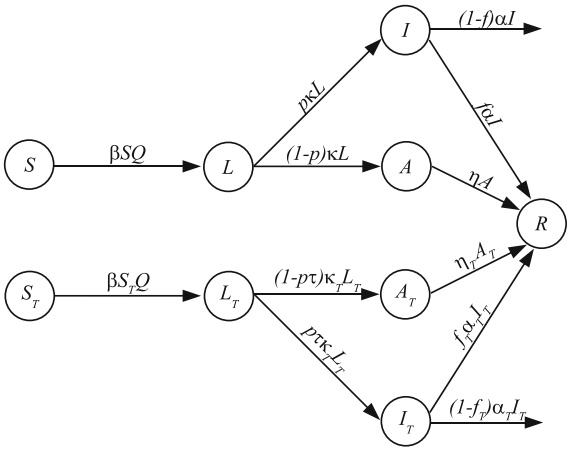

Fig. 9.2 Transition diagram corresponding to the vaccination model (9.5)

$$
\begin{aligned}
L_T' &= \sigma_S S_T \beta Q - \kappa_T L_T \\
I' &= p\kappa L - \alpha I \\
I_T' &= \tau p \kappa_T L_T - \alpha_T I_T \\
A' &= (1-p)\kappa L - \eta A \\
A_T' &= (1-p\tau)\kappa_T L_T - \eta_T A_T \\
R' &= \alpha I + \alpha_T I_T + \eta A + \eta_T A_T .
\end{aligned}
\tag{9.5}
$$

The initial conditions are

$$
\begin{aligned}
&S(0) = (1-\gamma)S_0, \quad S_T(0) = \gamma S_0, \quad I(0) = I_0, \quad N = S_0 + I_0, \\
&L(0) = L_T(0) = I_T(0) = A(0) = A_T(0) = 0
\end{aligned}
$$

corresponding to pre-epidemic treatment of a fraction γ of the population. A flow diagram for the model (9.5) is shown in Fig. 9.2.

Since the infection now is beginning in a population which is not fully susceptible, we speak of the control reproduction number $\mathscr{R}_c$ rather than the basic reproduction number. A computation using the next generation matrix leads to the control reproduction number

$$
\mathscr{R}_c = (1-\gamma)\mathscr{R}_u + \gamma \mathscr{R}_v,
$$

with

$$
\begin{aligned}
\mathscr{R}_u &= N\beta\Big[\frac{p}{\alpha} + \frac{\delta(1-p)}{\eta}\Big] = \mathscr{R}_0, \\
\mathscr{R}_v &= \sigma_S N\beta\Big[\frac{p\tau\sigma_I}{\alpha_T} + \frac{\delta(1-p\tau)\sigma_A}{\eta_T}\Big].
\end{aligned}
\tag{9.6}
$$

Then $\mathscr{R}_u$ is a reproduction number for unvaccinated people and $\mathscr{R}_v$ is a reproduction number for vaccinated people. There is a pair of final size relations for the two final sizes $S(\infty)$ and $S_T(\infty)$ in terms of the group sizes $N_u = (1-\gamma)N$, $N_v = \gamma N$, namely

$$\begin{aligned} \log \frac{(1-\gamma)S_0}{S_\infty} &= \mathscr{R}_u \left[1 - \frac{S_\infty}{N_u}\right] + \mathscr{R}_v \left[1 - \frac{S_T(\infty)}{N_v}\right], \\ \log \frac{\gamma S_0}{S_T(\infty)} &= \sigma_S \mathscr{R}_u \left[1 - \frac{S_\infty}{N_u}\right] + \mathscr{R}_v \left[1 - \frac{S_T(\infty)}{N_v}\right]. \end{aligned} \tag{9.7}$$

The number of symptomatic disease cases is

$$I_0 + p[(1-\gamma)S_0 - S(\infty)] + p\tau[\gamma S_0 - S_T(\infty)],$$

and the number of disease deaths is

$$(1-f)[I_0 + p(1-\gamma)S_0 - S(\infty)] + (1-f_T)p\tau[\gamma S_0 - S_T(\infty)].$$

These may be calculated with the aid of (9.7). By control of the epidemic we mean vaccinating enough people (i.e., taking γ large enough) to make $\mathscr{R}_c < 1$. We use the following parameters, suggested in [35] and [22],

$$\sigma_S = 0.3, \quad \sigma_I = \sigma_A = 0.2, \quad \kappa_T = 0.526, \quad \alpha_T = \eta_T = 0.323, \quad \tau = 0.4.$$

With these parameter values,

$$\mathscr{R}_u = 1.373, \quad \mathscr{R}_v = 0.047.$$

In order to make $\mathscr{R}_c = 1$, we need to take $\gamma = 0.28$. This is the fraction of the population that needs to be vaccinated to head off an epidemic.

We may solve the pair of final size equations with $S(0) = (1-\gamma)S_0$, $S_T(0) = \gamma S_0$ for $S(\infty)$, $S_T(\infty)$ for different values of γ. We do this for the parameter values suggested above and we obtain the results shown in Table 9.1, giving the treatment fraction γ, the number of untreated susceptibles $S(\infty)$ at the end of the epidemic, the number of treated susceptibles $S_T(\infty)$ at the end of the epidemic, the number of treated cases of influenza $I_0 + p[(1-\gamma)S_0 - S(\infty)]$, and the number of untreated cases $(\gamma S_0 - S_T(\infty)]$. The results indicate the benefits of pre-epidemic vaccination of even a small fraction of the population in reducing the number of influenza cases. They also demonstrate the advantage of vaccination to an individual. The attack rate in the vaccinated portion of the population is much less than the attack rate in the unvaccinated portion of the population.

Table 9.1 Effect of vaccination

Fraction treated	S_∞	$S_T(\infty)$	Untreated cases	Treated cases
0	1015	0	660	0
0.05	1079	84	552	4
0.1	1149	174	439	7
0.15	1224	271	323	7
0.2	1305	375	201	6
0.25	1395	487	76	3
0.3	1391	596	13	0

9.3 Antiviral Treatment

If no vaccine is available for a strain of influenza it would be possible to use an antiviral treatment. However, antiviral treatment affords protection only while the treatment is continued and is more expensive. In addition, antivirals are in short supply and expensive, and treatment of enough of the population to control an anticipated epidemic may not be feasible. A policy of treatment aimed particularly at people who have been infected or who have been in contact with infectives once a disease outbreak has begun may be a more appropriate approach. This requires a model with treatment rates for latent, infective, and asymptomatically infected members of the population that we construct building on the structure used for vaccination in (9.5).

Antiviral drugs have effects similar to vaccines in decreasing susceptibility to infection and decreasing infectivity, likelihood of developing symptoms, and length of infective period in case of infection. However, they are likely to be less effective than a well-matched vaccine, especially in the reduction of susceptibility.

Treatment may be given to diagnosed infectives. In addition, one may treat contacts of infectives who are thought to have been infected. This is modeled by treating latent members. In practice, some of those identified by contact tracing and treated would actually be susceptibles, but we neglect this in the model. Although we have allowed treatment of asymptomatics in the model, this is unlikely to be done, and we will describe the results of the model under the assumption $\varphi_A = \theta_A = 0$. However, for generality we retain the possibility of antiviral treatment of asymptomatics in the model. If treatment is given only to infectives, the compartments L_T, A_T are empty and may be omitted from the model.

We add to the model (9.5) antiviral treatment of latent, infective, and asymptomatically infected members of the population, but we do not assume an initial treated class. In addition to the assumptions made earlier we also assume

- There is a treatment rate φ_L in L and a rate θ_L of relapse from L_T to L, a treatment rate φ_I in I and a rate θ_I of relapse from I_T to I, and a treatment rate φ_A in A and a rate θ_A of relapse from A_T to A.

The resulting model is

$$\begin{aligned}
S' &= -\beta SQ \\
L' &= \beta SQ - \kappa L - \varphi_L L + \theta_L L_T \\
L'_T &= -\kappa_T L_T + \varphi_L L - \theta_L L_T \\
I' &= p\kappa L - \alpha I - \varphi_I I + \theta_I I_T \\
I'_T &= p\tau\kappa_T L_T - \alpha_T I_T + \varphi_I I - \theta_I I_T \\
A' &= (1-p)\kappa L - \eta A - \varphi_A A + \theta_A A_T \\
A'_T &= (1-p\tau)\kappa_T L_T - \eta_T A_T + \varphi_A A - \theta_A A_T \\
N' &= -(1-f)\alpha I - (1-f_T)\alpha_T I_T,
\end{aligned} \tag{9.8}$$

with Q as in (9.4). The initial conditions are

$$S(0) = S_0, \quad I(0) = I_0, \quad L(0) = L_T(0) = I_T(0) = A(0) = A_T(0) = 0, N = S_0 + I_0.$$

A flow diagram for the model (9.8) is shown in Fig. 9.3.

The calculation of $\mathscr{R}_c$ for the antiviral treatment model (9.8) is more complicated than for models considered previously, but it is possible to show that $\mathscr{R}_c = \mathscr{R}_I + \mathscr{R}_A$ with

$$\begin{aligned}
\mathscr{R}_I &= \frac{N\beta}{\Delta_I \Delta_L}\left[(\alpha_T + \theta_I + \sigma_I\varphi_I)p\kappa(\kappa_T + \theta_L) + (\theta_I + \sigma_I(\alpha + \varphi_I))p\tau\kappa_T\phi_L\right] \\
\mathscr{R}_A &= \frac{\delta N\beta}{\Delta_L}\left[\frac{(1-p)\kappa(\kappa_T + \theta_L)}{\eta} + \frac{\sigma_A(1-p\tau)\kappa_T\varphi_L}{\eta_T}\right],
\end{aligned} \tag{9.9}$$

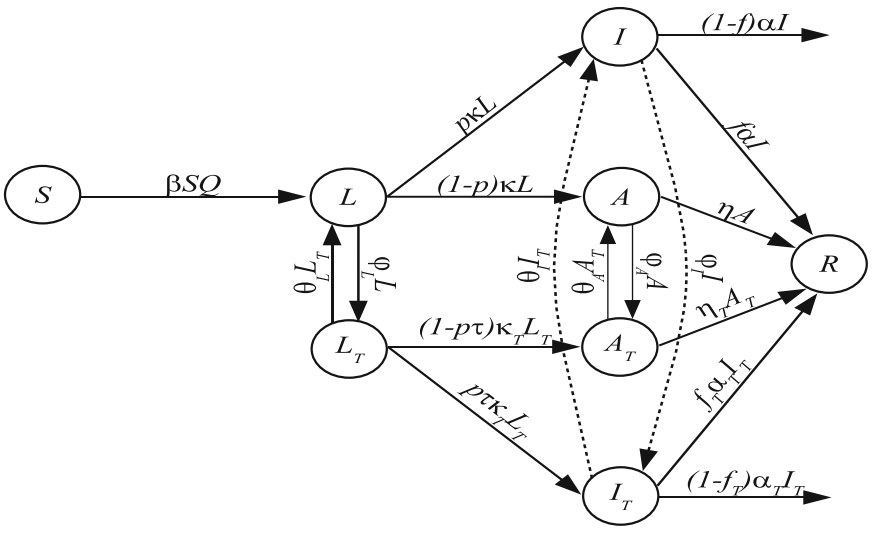

Fig. 9.3 Treatment model (9.8)

where

$$\Delta_I = (\alpha + \varphi_I)(\alpha_T + \theta_I) - \theta_I \varphi_I$$
$$\Delta_L = (\kappa + \varphi_L)(\kappa_T + \theta_L) - \theta_L \varphi_L.$$

The final size equation is

$$\log \frac{S_0}{S_\infty} = \mathscr{R}_c \left[1 - \frac{S_\infty}{S_0} \right] + \frac{\beta I_0 (\alpha_T + \theta_I + \sigma_I \varphi_I)}{\Delta_I}. \tag{9.10}$$

The number of people treated is

$$\int_0^\infty [\varphi_L L(t) + \varphi_I I(t)] dt$$

and the number of disease cases is

$$I_0 + \int_0^\infty [p\kappa L(t) + p\tau\kappa_T L_T] dt$$

which can be evaluated in terms of the parameters of the model. The number of people treated and the number of disease cases are constant multiples of $S_0 - S_\infty$ plus constant multiples of the (presumably small) number of initial infectives. Since the expressions in terms of $S_0 - S_\infty$ and I_0 are more complicated than in the cases of no treatment or vaccination, we have chosen to give these numbers in terms of integrals.

There is an important consequence of the calculation of the number of disease cases and treatments that is not at all obvious. If $\mathscr{R}_c$ is close to 1 or ≤ 1, $S_0 - S_\infty$ depends very sensitively on changes in I_0. For example, in a population of 2000 with $\mathscr{R}_0 = 1.5$, a change in I_0 from 1 to 2 multiplies $S_0 - S_\infty$ and therefore treatments and cases by 1.4 and a change in I_0 from 1 to 5 multiplies $S_0 - S_\infty$ and therefore treatments and cases by 3. Thus, numerical predictions in themselves are of little value. However, comparison of different strategies is valid, and the model indicates the importance of early action while the number of infectives is small.

In the special case that treatment is applied only to infectives, $\mathscr{R}_c$ is given by the simpler expression

$$\mathscr{R}_c = N\beta \left[\frac{p(\alpha_T + \theta_I + \sigma_I \varphi_I)}{\Delta_I} + \frac{\delta(1-p)}{\eta} \right].$$

The number of disease cases is $I_0 + p(S_0 - S_\infty)$, and the number of people treated is

$$\frac{\varphi_I(\alpha_T + \theta_I)}{\Delta_I} [I_0 + p(S_0 - S_\infty)].$$

Since the infective period is short, antiviral treatment would normally be applied as long as the patient remains infective. Thus we assume $\theta_I = 0$, and these relations become even simpler. The control reproduction number is

$$\mathscr{R}_c = N\beta\left[\frac{p(\alpha_T + \sigma_I\varphi_I)}{\alpha_T(\alpha + \varphi_I)} + \frac{\delta(1-p)}{\eta}\right], \tag{9.11}$$

and the number of people treated is

$$\frac{\varphi_I}{\alpha + \varphi_I}[I_0 + p(S_0 - S_\infty)]. \tag{9.12}$$

Since the basic reproduction number of a future pandemic cannot be known in advance, it is necessary to take a range of contact rates in order to make predictions. In particular, we could compare the effectiveness in controlling the number of infections or the number of disease deaths of different strategies such as treating only infectives, treating only latent members, or treating a combination of both infective and latent members. In making such comparisons, it is important to take into account that treatment of latent members must be supplied for a longer period than for infectives. In case of a pandemic, there are also questions of whether the supply of antiviral drugs will be sufficient to carry out a given strategy. For this reason, we must calculate the number of treatments corresponding to a given treatment rate. It is possible to do this from the model; the result is a constant multiple of I_0 plus a multiple of $S_0 - S_\infty$.

The results of such calculations appear to indicate that treatment of diagnosed infectives is the most effective strategy [6, 7]. However, there are other considerations that would go into any policy decision. For example, a pandemic would threaten to disrupt essential services and it could be decided to use antiviral drugs prophylactically in an attempt to protect health care workers and public safety personnel. A study including this aspect based on the antiviral treatment model given here is reported in [26].

For simulations, we use the initial values

$$S_0 = 1988, \quad I_0 = 12,$$

the parameters of Sect. 9.1, and for antiviral efficacy we assume

$$\sigma_S = 0.7, \quad \sigma_I = \sigma_A = 0.2,$$

based on data reported in [50].

We simulate the model (9.8) with $\theta_I = 0$, assuming that treatment continues for the duration of the infection. We assume that 80% of diagnosed infectives are treated within 1 day. Since the assumption of treatment at a constant rate φ_I implies treatment of a fraction $1 - exp(-\varphi_I t)$ after a time t, we take φ_I to satisfy

$$1 - e^{-\varphi_I} = 0.8,$$

Table 9.2 Control by antiviral treatment

βN	$\mathscr{R}_0$	$\mathscr{R}_c$	Disease cases	Treatments
0.402	1.37	0.92	64	56
0.435	1.49	1.00	130	113
0.5	1.71	1.15	373	314
0.7	2.39	1.61	865	751

or $\varphi_I = 1.61$. We use different values of βN, corresponding to different values of $\mathscr{R}_0$, and use (9.10) and (9.11), obtaining the results shown in Table 9.2.

We calculate from (9.11) that $\mathscr{R}_c = 1$ for an attack rate of 39%. This is the critical attack rate beyond which treatment at the rate specified cannot control the pandemic.

9.4 Seasonal Influenza Epidemics

There are annual influenza outbreaks, usually in the fall and winter. Currently, the annual influenza outbreak is the subtype H3N2, coexisting with the subtype H1N1. Influenza A viruses are divided into subtypes identified by two proteins on the surface of the virus, namely hemagglutinin (HA) and neuraminidase (NA). The designation H3N2 means an influenza A virus that has an HA3 protein and an NA2 protein. An influenza virus undergoes antigenic drift, rapid minor genetic variation in a currently circulating subtype. Recovery from an influenza virus confers immunity against reinfection, but antigenic drift means that a later contact with an influenza virus of the same subtype will mean only partial immunity against infection. Until now, we have studied influenza epidemics in isolation, but if there is a seasonal outbreak of a strain that has been occurring for several seasons part of the population will have some cross-immunity protecting against another infection. Models for recurring seasonal outbreaks taking this into account have been analyzed by Andreasen et al. [3, 4]. Thus we now assume that at the beginning of a seasonal influenza outbreak individuals have a level of cross-immunity depending on the most recent outbreak, up to a maximum of n seasons.

We assume that cross-immunity reduces both susceptibility to infection and infectivity in case of infection. At the beginning of a seasonal outbreak, we assume that all hosts are susceptible and we let N_i denote the number of hosts whose last infection occurred i seasons ago and we include in N_n all who have never been infected. We are dividing the total population into n sub-populations $(N_1, N_2, \cdots, N_n)$ representing the distribution of cross immunities at the start of a seasonal epidemic. The (constant) total population size is

$$N = \sum_{i=1}^{n} N_i.$$

For simplicity, we assume that during a seasonal epidemic the model is a simple SIR model, ignoring the latent period and the existence of asymptomatic cases.

Thus for each class i we have I_i infectious and R_i recovered individuals. The transmission dynamics are given by the system

$$\begin{aligned} S_i' &= -\sigma_i S_i \beta \sum_{j=1}^{n} \tau_j I_j \\ I_i' &= \sigma_i S_i \beta \sum_{j=1}^{n} \tau_j I_j - \alpha I_i \\ R_i' &= \alpha I_i . \end{aligned} \tag{9.13}$$

Here α is the recovery rate, β is the transmission coefficient in the absence of cross-immunity, σ_i is the relative susceptibility of individuals whose last infection occurred i seasons ago, and τ_i is the relative infectivity of individuals whose last infection occurred i seasons ago. It is reasonable to assume that cross-immunity fades with time, so that

$$0 \le \sigma_1 \le \sigma_2 \le \cdots \le \sigma_n = 1, \quad 0 \le \tau_1 \le \tau_2 \le \cdots \le \tau_n = 1.$$

If we define the total infectivity

$$\varphi(t) = \sum_{j=1}^{n} \tau_j I_j,$$

we may rewrite the model (9.13) as

$$\begin{aligned} S_i' &= -\sigma_i \beta S_i \varphi \\ I_i' &= \sigma_i \beta S_i \varphi - \alpha I_i . \end{aligned} \tag{9.14}$$

There is a disease-free equilibrium $S_i = N_i$, $I_i = 0 (i = 1, 2, \cdots, n)$.

The next generation matrix is

$$K = \frac{\beta}{\alpha} \begin{bmatrix} \sigma_1 N_1 \tau_1 & \sigma_2 N_1 \tau_1 & \cdots & \sigma_n N_1 \tau_1 \\ \sigma_2 N_2 \tau_1 & \sigma_2 N_2 \tau_2 & \cdots & \sigma_n N_2 \tau_2 \\ \vdots & \vdots & \ddots & \vdots \\ \sigma_n N_n \tau_1 & \sigma_n N_n \tau_2 & \cdots & \sigma_n N_n \tau_n \end{bmatrix}.$$

Now, if P is the diagonal matrix with diagonal entries $\sigma_i N_i, 1 \le i \le n$, the matrix $P^{-1} K P$ similar to K has every row β/α multiplied by $(\sigma_1 \tau_1 N_1, \sigma_2 \tau_2 N_2, \cdots, \sigma_n \tau_n N_n)$ and therefore has rank 1. This implies that all but one of the eigenvalues of K are zero, and the remaining eigenvalue is equal to the trace of K. From this we conclude that the spectral radius of K is equal to the trace of K and the control reproduction number of the cross-immunity model (9.14) is

$$\mathscr{R}_S = \frac{\beta}{\alpha} \sum_{i=1}^{n} \sigma_1 \tau_1 N_i. \tag{9.15}$$

If there were no cross-immunity, the basic reproduction number would be

$$\mathscr{R}_0 = \frac{\beta N}{\alpha}.$$

Because $(S_i + I_i)' = -\alpha I_i$, we can deduce as in Sect. 2.4 that

$$\lim_{t\to\infty} I_i(t) = 0, \quad \lim_{t\to\infty} S_i(t) = S_i(\infty),$$

and

$$\alpha \int_0^\infty I_i(t)dt = N_i - S_i(\infty),$$

using $S_i(0) + I_i(0) = N_i$. Integration of the first equation of (9.14) gives

$$\begin{aligned} \log \frac{N_i}{S_i(\infty)} &= \beta\sigma_i \int_0^\infty \varphi(t)dt \\ &= \beta\sigma_i \sum_{j=1}^{n} \tau_j \int_0^\infty I_j(t)dt \\ &= \frac{\beta}{\alpha}\sigma_i \sum_{j=1}^{n} \tau_j [N_j - S_j(\infty)] \\ &= \sigma_i \sum_{j=1}^{n} \tau_j \frac{\beta N_j}{\alpha} \left[1 - \frac{S_j(\infty)}{N_j}\right]. \end{aligned} \tag{9.16}$$

We can write this final size relation in terms of the single unknown $S_n(\infty)$ because from (9.14) and $\sigma_n = 1$ we have

$$\frac{S_i'}{S_i} = \sigma_i \frac{S_n'}{S_n},$$

and integration gives

$$\frac{S_i(\infty)}{N_i} = \left[\frac{S_n(\infty)}{N_n}\right]^{\sigma_i}. \tag{9.17}$$

Substitution of (9.17) into (9.16) gives a relation for $S_n(\infty)$, namely

$$\log \frac{N_n}{S_n(\infty)} = \sigma_n \sum_{j=1}^{n} \tau_j \frac{\beta N_j}{\alpha} \left[1 - \left(\frac{S_n(\infty)}{N_n} \right)^{\sigma_j} \right].$$

Then (9.17) gives solutions for $S_i(\infty), i = 1, \ldots, n-1$.

9.4.1 Season to Season Transition

The above analysis traces the development of a seasonal epidemic. We assume that at the beginning of the next season's epidemic, the final compartment sizes give the separation of the population into new cross-immunity groups $(N_1^*, N_2^*, \ldots, N_n^*)$. The individuals who were infected during the previous season's epidemic form the new group N_1^*, and the remaining individuals from N_i move to N_{i+1}^*. Thus

$$\begin{aligned} N_1^* &= N - \sum_{i=1}^{n} S_i(\infty) \\ N_j^* &= S_{j-1}(\infty), \quad j = 2, \cdots, n-1 \\ N_n^* &= S_{n-1}(\infty) + S_n(\infty). \end{aligned}$$

This relation describes the transition from one seasonal epidemic to the next. The severity of one season's epidemic affects the cross-immunity for the next season's epidemic. If the seasonal epidemic 1 year is severe, then because there is more cross-immunity the next year it is reasonable to expect a less severe epidemic the next year.

9.5 Pandemic Influenza

In some years, there is an immunological change that produces a new subtype. Such a change is called an antigenic shift, and is usually a result of recombination of gene segments from viruses circulating in humans with virus segments from avian viruses. Since this subtype is new, humans have little or no immunity against it, and the result often is a pandemic. For example, the H1N1 subtype emerged in the pandemic influenza of 1918 and circulated until 1957. In the pandemic of 1957 a new subtype, H2N2, emerged and replaced H1N1. In the pandemic of 1968, H3N2 replaced the prevailing subtype H2N2. In 1977, H1N1 was reintroduced and has been circulating along with H3N2 since then. A natural question is whether a new pandemic strain will replace the currently circulating subtype or coexist with it. To study this question, we must model a pandemic following a seasonal influenza outbreak and then model the next seasonal outbreak. This is necessary because there may be some cross-immunity between the seasonal and pandemic subtypes. The interplay between seasonal and pandemic influenza has been studied by Asaduzzaman et al. [8].

9.5.1 A Pandemic Outbreak

We begin by assuming that there has been a seasonal influenza epidemic and that at the end of this epidemic the population of total size N is divided into cross-immunity sub-populations with respect to the seasonal epidemics of sizes $(N_1, N_2, \cdots, N_n)$. We assume that there is a cross-immunity between the pandemic strain and the seasonal strain, for individuals in the population who have recovered from the seasonal strain in the previous n seasonal outbreaks reducing susceptibility by a factor ρ, $(0 \leq \rho \leq 1)$. Thus $\rho = 0$ corresponds to full cross-immunity and $\rho = 1$ corresponds to no cross-immunity. Then the model for pandemic influenza is

$$\begin{aligned} S_i' &= -\rho\tilde{\beta} S_i I, \quad i = 1, 2, \cdots, n-1 \\ S_n' &= -\tilde{\beta} S_n I \\ I' &= \tilde{\beta}\Big[\rho(S_1 + S_2 + \cdots + S_{n-1}) + S_n\Big] I - \alpha I. \end{aligned} \tag{9.18}$$

If there were no cross-immunity, the basic reproduction number would be

$$\tilde{\mathscr{R}}_0 = \frac{\tilde{\beta} N}{\alpha}, \tag{9.19}$$

where $\tilde{\beta}$ is the pandemic contact rate.

An analysis very similar to that of Sect. 9.5 shows that the pandemic reproduction number is

$$\mathscr{R}_P = \frac{\tilde{\beta}}{\alpha}\Big[\rho(N_1 + N_2 + \cdots + N_{n-1}) + N_n\Big] = \frac{\rho\tilde{\beta} N}{\alpha} + \frac{(1-\rho)\tilde{\beta} N_n}{\alpha},$$

an increasing function of ρ. If $\mathscr{R}_P > 1$, there will be a pandemic.

We assume that the pandemic would invade if there were no cross-immunity, that is,

$$\tilde{\mathscr{R}}_0 > 1.$$

Also, again much as in Sect. 9.5, we obtain a final size relation

$$\begin{aligned} \log \frac{N_n}{S_n(\infty)} &= \frac{\tilde{\beta} N}{\alpha}\left[1 - \frac{\sum_{i=1}^{n} S_i(\infty)}{N}\right] \\ \frac{S_i(\infty)}{N_i} &= \left[\frac{S_n(\infty)}{N_n}\right]^{\rho}, \quad i = 1, \cdots, n-1. \end{aligned} \tag{9.20}$$

This relation gives the cross-immunity distribution for the pandemic. When we model the seasonal epidemic following the pandemic, we will need this result in order to distinguish between individuals susceptible to the seasonal influenza

virus having cross-immunity to the pandemic strain and individuals without cross-immunity.

9.5.2 Seasonal Outbreaks Following a Pandemic

In order to model a seasonal outbreak following a pandemic, because of cross-immunity between the seasonal and pandemic viruses, we must divide each of the subgroups $(N_1, N_2, \cdots, N_n)$ into two parts, depending on whether the members of the group were infected by the pandemic. Now, we let M_i denote the individuals whose most recent seasonal infection was i seasons ago and who escaped the pandemic, and let $\tilde{M}_i$ denote the individuals whose most recent seasonal infection was i seasons ago and who were infected in the pandemic. Then $N_i = M_i + \tilde{M}_i$. We denote by S_i the number of individuals in M_i susceptible to the seasonal influenza (who escaped the pandemic influenza) and by $\tilde{S}_i$ the number of individuals in M_i susceptible to the seasonal influenza (infected by the pandemic). Taking into account the cross-immunity of individuals in M_i and again defining the total infectivity

$$\varphi(t) = \sum_{j=1}^{n} \tau_j I_j,$$

we obtain the model

$$\begin{aligned} S_i' &= -\sigma_i \beta S_i \varphi \\ \tilde{S}' &= -\rho\sigma_i \tilde{S}_i \varphi \\ I_i' &= \sigma_i \beta (S_i + \rho \tilde{S}_i)\varphi - \alpha I_i. \end{aligned} \tag{9.21}$$

The calculation of the reproduction number is again much the same as in Sect. 9.4, and yields the result

$$\mathscr{R} = \frac{\beta}{\alpha} \sum_{i=1}^{n} \sigma_i \tau_i (M_i + \rho \tilde{M}_i).$$

In order to evaluate this, we need to determine M_i and $\tilde{M}_i$ from the final size relation (9.20). We have $M_i = S_i(\infty)$, $\tilde{M}_i = N_i - S_i(\infty)$, so that

$$M_i + \rho \tilde{M}_i = M_i(1-\rho) + \rho N_i,$$

with $S_i(\infty)$ given by (9.20). If we let $x = \frac{S_n(\infty)}{N_n}$, then (9.20) gives

$$
\begin{aligned}
-\log x &= \frac{\tilde{\beta}}{\alpha}[N - \sum_{i=1}^{n} S_i(\infty)] \\
&= \frac{\tilde{\beta}N}{\alpha}\left[1 - \frac{N_1 S_n^{\rho} + N_2 S_n^{\rho} + \cdots + N_n S_n^{\rho}}{N N_n^{\rho}}\right] \\
&= \frac{\tilde{\beta}N}{\alpha}[1 - x^{\rho}].
\end{aligned}
\tag{9.22}
$$

Consider the function

$$
f(x) = \log x + \frac{\tilde{\beta}N}{\alpha}[1 - x^{\rho}] = \log x + \tilde{\mathscr{R}}_0[1 - x^{\rho}],
$$

where $\tilde{\mathscr{R}}_0$ is given by (9.19). A solution x of (9.22) is epidemiologically meaningful only if $x < 1$; otherwise, the pandemic does not invade. The value $x = 1$ is always a root of (9.22); the pandemic invades if and only if there is a second root less than 1. The function $f(x)$ is negative for x close to 0. If $\rho\tilde{\mathscr{R}} < 1$, $f(x)$ is monotone increasing for $0 < x \leq 1$ and therefore there is no second root of (9.22) less than 1. Thus, if $\rho\tilde{\mathscr{R}}_0 < 1$, the pandemic does not invade. On the other hand, if $\rho\tilde{\mathscr{R}}_0 > 1$, $f'(1) < 0$, and there must be a second root of (9.22). The pandemic invades if and only if $\rho\tilde{\mathscr{R}}_0 > 1$.

Now, the reproduction number is

$$
\begin{aligned}
\mathscr{R} &= \frac{\beta}{\alpha}\sum_{i=1)}^{n} \sigma_i \tau_i [(1-\rho)N_i x^{\rho} + \rho N_i] \\
&= \frac{\beta}{\alpha}(1-\rho)\sum_{i=1}^{n} \sigma_i \tau_i N_i x^{\rho} + \frac{\beta}{\alpha}\rho \sum_{i=1}^{n} \sigma_i \tau_i N_i.
\end{aligned}
\tag{9.23}
$$

If $\mathscr{R}$, with x given as a function of ρ by (9.22), is greater than 1, then the pandemic and seasonal strains will coexist, but if $\mathscr{R} < 1$, then the pandemic strain will replace the seasonal strain.

We assume that the seasonal epidemic would take place if there were no pandemic strain present, that is,

$$
\mathscr{R}_S > 1.
$$

For $\rho = 1$ (no cross-immunity) we have

$$
\mathscr{R} = \mathscr{R}_S > 1,
$$

and this means that the pandemic and seasonal strains coexist. For $\rho = 1/\tilde{\mathscr{R}}_0$, $x = 1$, and

$$\mathscr{R} = \frac{\beta}{\alpha} \sum_{i=1}^{n} \sigma_i \tau_i N_i = \mathscr{R}_S > 1,$$

and the pandemic and seasonal strains coexist.

Numerical simulations indicate that $\mathscr{R} < 1$ for some values of ρ between $1/\tilde{\mathscr{R}}_0$ and 1, which implies that for some values of ρ the pandemic strain will replace the seasonal strain.

9.6 The Influenza Pandemic of 2009

In the spring of 2009 a new strain (H1N1) of influenza A was developed, apparently first in Mexico, and spread rapidly through much of the world. Initially, it was thought that there was no resistance to this strain, although it developed later that people who were old enough to have been exposed to similar strains in the 1950s appeared to be less susceptible than younger people. It also appeared initially that this strain had a high case fatality rate, but it was learned later that since many cases were mild enough not to be reported the early data were weighted towards severe cases. The case fatality rate was actually lower than for most seasonal influenza strains.

Management of the H1N1 influenza pandemic of 2009 made use of mathematical models and the experience gained from previous epidemics, but also exposed some gaps between a well-developed mathematical theory of epidemics and real-life epidemics, notably in the acquisition of reliable data early in the pandemic, understanding of spatial spread of a pandemic, and the development of multiple epidemic waves.

There are important differences in the kinds of models of value to different types of scientists. There are *strategic* disease transmission models aimed at the understanding of broad general principles, and *tactical* models with the goal of helping make decisions in specific and detailed situations on short-term policies. A model that predicts how many people will become ill in an anticipated epidemic is quite different from a model that helps to identify which subgroups of a population should have highest priority for preventive vaccination with an uncertain prediction of how much vaccine will be available in a given time frame.

9.6.1 A Tactical Influenza Model

There was a second wave of infections in the 2009 H1N1 influenza pandemic, just as in several previous influenza pandemics. As soon as possible, during the first wave, work began on the development of a vaccine matched to the virus to be used to combat the expected second wave [41]. Since a vaccine requires at least 6 months

for development, and the second wave could begin within 6 months of the first wave, there was an urgent need to prepare a vaccine distribution strategy.

In this section, we describe the model of [18] as an example of a tactical model. This model was used by the BC Center for Disease Control in making planning decisions for vaccination distribution during the second wave of the 2009 H1N1 influenza pandemic. Because of the need to make such decisions rapidly, the development and application of the model was more urgent than the writing of the paper that described the work, and use of the results preceded the write-up. In a pandemic, there is still much to be done after the model has been developed and applied, and frequently there is no time to explore basic theoretical questions that may arise in the study. Ideally, these questions can be studied in more depth after the urgency of coping with a pandemic has passed, and this is an opportunity to return to more general strategic models.

Infection rates in an influenza epidemic depend strongly on the (demographic) age of the individuals in contact. This dependence of transmission and infection rates on age (the age profile) may vary significantly between locations and from year to year for seasonal epidemics. Also, the age profile in a pandemic is probably unlike that for seasonal epidemics. For this reason, real-time planning during an epidemic must make use of surveillance data obtained as soon as possible after the epidemic has begun. The data gathered during the first wave in the spring of 2009 were used to project the age profile to be expected in the second wave. A compartmental model with 6 compartments in each of the 40 population subgroups, covering 8 age classes and 5 activity levels using this age profile and existing estimates of the Vancouver contact network structure, was developed to project the results of different vaccination strategies.

The analysis of the model was carried out using numerical simulations, because comparisons of different strategies, including numerical estimates of disease cases and vaccine quantities required, were needed quickly and because general theoretical analysis of this high-dimensional system would have been too complicated. The numerical simulations indicated that a good estimate of the epidemic peak would be essential for making policy decisions on vaccination strategies. In a pandemic situation, delays in vaccine production may mean that vaccination cannot be started until an epidemic is already underway, and the model suggested that an early start to vaccine distribution makes a big difference in the effectiveness of the vaccination program. This raises a general theoretical question of the relation between the starting time of vaccination and the effectiveness of the vaccination program. Future theoretical study of models of this type would be very useful for planning vaccination strategies for epidemics in the future.

9.6.2 Multiple Epidemic Waves

During the 1918 “Spanish flu” pandemic, North America and much of Western Europe experienced two waves of infection with the second wave more severe than

the first [20, 21]. Unlike seasonal influenza epidemics, which occur at predictable times each year, influenza pandemics are often shifted slightly from the usual "influenza season" and have multiple waves of varying severity. This suggests a modeling question that does not arise with seasonal influenza. During a first wave of a pandemic it should be possible to isolate virus samples and begin development of a vaccine matched to the virus in time to allow vaccination against the virus that could help to manage a second wave. One question that arises is prediction of the timing of a second wave. This is not yet possible because there is not yet a satisfactory explanation of the causes of a second wave. One suggestion that has been made is that transmissibility of virus varies seasonally, and this has been used to try to predict whether an endemic disease will exhibit seasonal outbreaks [44, 45]. The same approach can be used to formulate an SIR epidemic model with a periodic contact rate that can exhibit two epidemic waves [12]. However, the behavior of such a model depends strongly on the timing of the epidemic. If we assume that the contact rate is highest in the winter, lowest in the summer, and varies sinusoidally with a period of 1 year, we could use a simple SIR model with a variable contact rate. With N as the (constant) total population size, this suggests a model

$$\begin{aligned} S' &= -\beta(t)\frac{SI}{N} \\ I' &= \beta(t)\frac{SI}{N} - \alpha I, \end{aligned} \tag{9.24}$$

where

$$\beta(t) = \beta\left[1 + c\cos\left(\frac{\pi(t+t_0)}{180}\right)\right],$$

with parameter values

$$\begin{aligned} &\alpha = 0.25, \quad \beta = 0.45, \quad c = 0.45, \\ &N = 1000, \quad S_0 = 999, \quad I_0 = 1, \quad t_0 = 85, 90, 95. \end{aligned}$$

The choice of t_0 determines where in the oscillation of $\beta(t)$ the epidemic begins, because at the start of the epidemic ($t = 0$)

$$\beta(0) = \beta\left[1 + c\cos\left(\frac{\pi t_0}{180}\right)\right].$$

Thus t_0 is the number of days after the maximum transmissibility that the epidemic begins. By numerical integration of (9.24), we obtain the following three epidemic curves (giving the number of infective individuals as a function of time), with the same parameters except that by varying t_0 the starting date of the epidemic is moved 5 days later from one curve to the next.

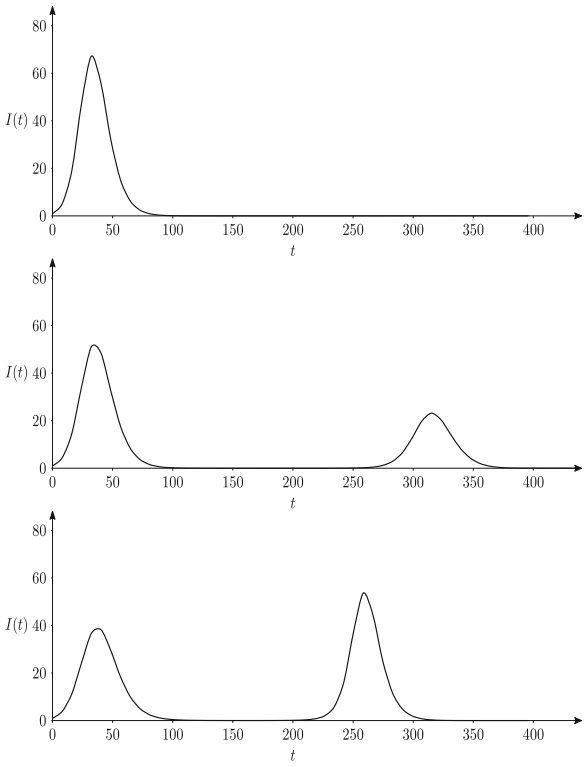

Fig. 9.4 Top: A one-wave epidemic curve, $t_0 = 85$. Middle: A two-wave epidemic curve, first wave more severe, $t_0 = 90$. Bottom: A two-wave epidemic curve, second wave more severe, $t_0 = 95$

An interpretation of these curves is that if the epidemic begins when the contact rate is decreasing and is close to its minimum value and the contact rate is relatively small over the course of the epidemic, the wave may end while there are still enough susceptibles to support a second wave when the contact rate increases, as in Fig. 9.4 (middle and bottom plots). However, if the epidemic begins earlier it may continue until enough individuals are infected that a second wave cannot be supported even when the contact rate becomes large, as in the top plot of Fig. 9.4.

Simulations indicate that for the model (9.24) with the parameter values used here there is a small window of starting times corresponding to the interval $90 \leq t_0 \leq 110$ for which a second wave is possible. The nature of the epidemic curves indicates that the behavior depends critically on timing and this means that such a model is not suitable for precise predictions. Note that there may be a single wave or two waves, and if there are two waves either one may be more severe. Not only does the prediction depend on the timing of the introduction of infection, but this timing is stochastic, and by its very nature unpredictable. It depends on mutations of the virus and importations of new cases.

We have here a strategic model that predicts the possibility of a second wave, but this is not sufficient to be confident about using it to advise policy, because we do not have enough evidence to be sure about the cause of a second wave. Before

we could make predictions we need more evidence about factors that could cause a second wave and more detailed tactical models, including sensitivity analysis. Another factor that has been suggested as a possible explanation for a second epidemic wave is coinfection with other respiratory infections that might increase susceptibility, and some experimental data would be needed that might confirm or deny that either seasonal variation in transmission or coinfection, or both, could explain multiple pandemic waves. In the H1N1 influenza pandemic of 2009, there were some concerns about the development of drug resistance as a consequence of antiviral treatment. While this did not appear to have widespread consequences, in a more severe disease outbreak in which more patients receive antiviral treatment there could be major effects. The modeling of drug resistance effects in an influenza pandemic has begun [1, 5, 36, 42, 43], but much more needs to be understood. A full analysis of the development of drug resistance will require nested models including immunological in-host aspects as well as effects on the population level.

Data from the 1918 pandemic indicate clearly that behavioral response, both individual and public health measures, had significant effects on the outcome of the epidemic [9]. Incorporating behavioral responses is a new aspect of epidemic modeling, and there is much to be learned about the factors that influence behavioral responses when a disease outbreak begins.

9.6.3 Parameter Estimation and Forecast of the Fall Wave

The model predictions included in this section are presented in [47]. With the recognition of a new, potentially pandemic strain of influenza A(H1N1) in April 2009, the laboratories at the US CDC and the World Health Organization (WHO) dramatically increased their testing activity from week 17 onwards (week ending 2 May 2009), as can be seen in Fig. 9.5. In this analysis, we use the extrapolation of a model fitted to the confirmed influenza A(H1N1)v case counts during summer 2009 to predict the behavior of the pandemic during autumn 2009.

The following model with seasonally forced transmission is used:

$$\begin{aligned} S' &= -\beta(t)\,\frac{SI}{N} \\ I' &= \beta(t)\,\frac{SI}{N} - \alpha I, \end{aligned} \tag{9.25}$$

where $N = 305{,}000{,}000$ denote the total population in the United States (US). The R equation is omitted as it can be determined by $R = N - S - I$. The transmission rate is chosen to be

$$\beta(t) = \beta_0 + \beta_1 \cos(\pi t/180), \tag{9.26}$$

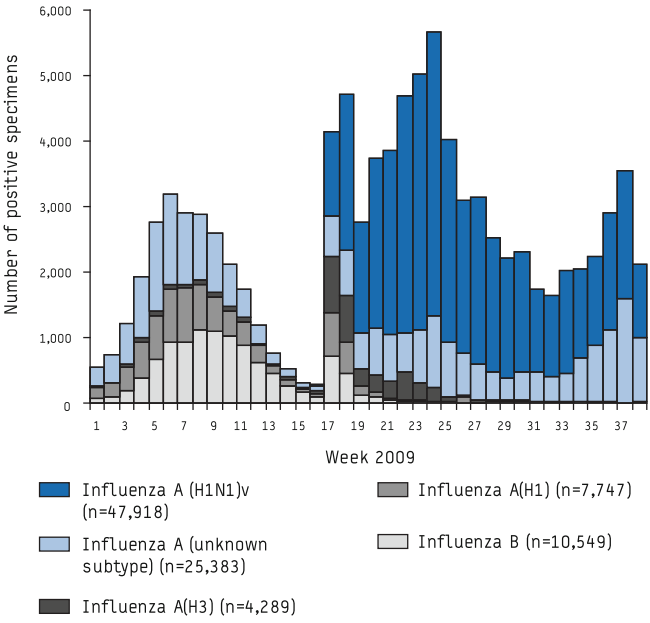

US CDC: United States Centers for Disease Control and Prevention; NREVSS: National Respiratory and Enteric Virus Surveillance System; WHO: World Health Organization.

Fig. 9.5 Influenza-positive tests reported to the US CDC by US WHO/NERVSS-collaborating laboratories, national summary, United States, 2009 until 26 September

where β_0 and β_1 are constants to be estimated from data. Assume that $I(t_0) = 1$, where t_0 is the initial time, which is another parameter to be estimated from data. The parameter α is chosen so that the infective period is $1/\alpha = 3$ days.

The three parameters (β_0, β_1, t_0) were estimated using the data shown in Fig. 9.5 on influenza-positive tests reported to the US CDC by US WHO/NREVSS-collaborating laboratories, national summary, United States, 2009 until 26 September. To avoid bias due to increased testing for H1N1 around week 16, only data from week 21 to 33 (from 24 May to 22 August 2009) were used. From the past experience with influenza, the lower and upper bounds were chosen to be $\beta_0 \in (0.92\alpha, 2.52\alpha)$ and $\beta_1 \in (0.05\alpha, 0.8\alpha)$, and $t_0 \in (-8, 10)$ (weeks relative to the beginning of 2009). The best estimates were determined by fitting the model to data, and the parameter values that provided the best Pearson chi-square statistics are listed in Table 9.3.

Using the estimated parameter values, forecast of the time and size of the fall wave was produced by simulating the model under two scenarios: one is without vaccination and the other included the planned CDC vaccination program, which would begin with six to seven million doses being delivered by the end of the first full week in October (week 40), with 10–20 million doses being delivered

Table 9.3 Estimates of parameters for the 2009 H1N1 model

Parameter	Value	95% confidence interval
β_0	1.56	(1.43, 1.77)
β_1	0.54	(0.39, 0.54)
t_0	24 February	(8 February, 7 March)

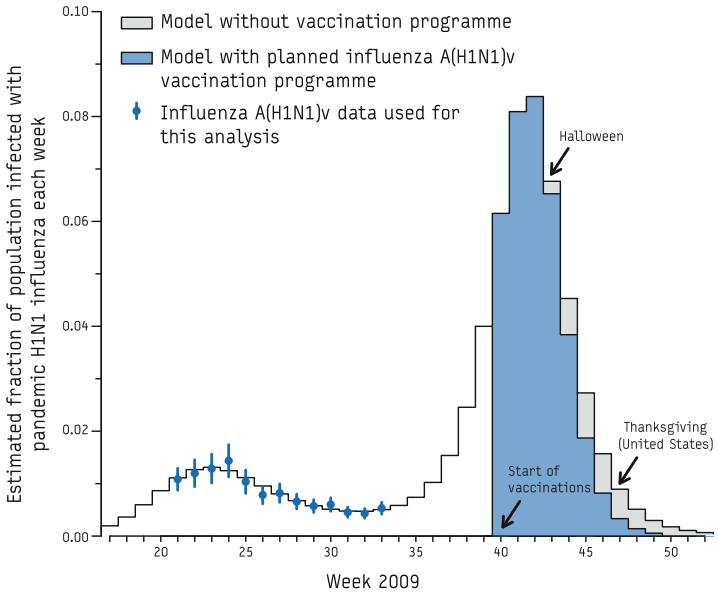

Fig. 9.6 Prediction for the 2009 H1N1 pandemic in the US using model (9.25)

weekly thereafter. It is assumed that for healthy adults, full immunity to H1N1 influenza is achieved about 2 weeks after vaccination with one dose of vaccine [30, 37]. For simulations of the model when vaccinations are incorporated, the number of susceptible individuals in the simulations was decreased according to the appropriate proportion of immune due to vaccination. The simulation outcomes are presented in Fig. 9.6.

In Fig. 9.6, the curves associated with the darker and lighter areas correspond to the cases of with and without vaccination. The model predicts that in the absence of vaccine, the peak wave of infection will occur near the end of October in week 42 (95% CI: week 39, 43). By the end of 2009, the model predicts that a total of 63% of the population will have been infected (95% CI: 57%, 70%). For the case when the planned vaccination program is considered, the model results suggest that a relative reduction of about 6% in the total number of people infected with influenza A(H1N1)v virus by the end of the year 2009 (95% CI: 1%, 17%).

The most striking feature of the model is that it accurately predicted the peak time of the pandemic. According to CDC 2009 H1N1 confirmed case count data (see [17]), the peak of the fall wave was reached at the end of October (which is between weeks 42 and 43, see the left-hand plot in Fig. 9.7), which is consistent with

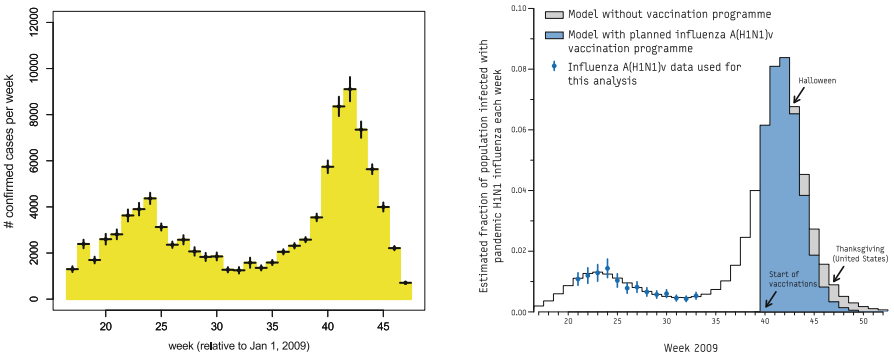

Fig. 9.7 The left figure illustrates the CDC 2009 confirmed H1N1 count data (the error bars represent variations calculated by the proposers that account for US regional variability in the timing of the pandemic). The right figure shows predictions by our model in [47]

our model result. It is worth noting that the model used in the analysis is a simple SIR model with a seasonally forced infection rate. Although further examinations are certainly needed to study the applicability of the modeling approach to general scenarios, the model results in this analysis demonstrated clearly the advantage and capability of mathematical models in understanding disease dynamics.

9.7 *An SIQR Model with Multiple Strains with Cross-Immunity

It was during the *Black Death* in the twentieth century in Venice that a system of quarantine was first put in operation. It demanded ships to lay at anchor for "40 days" (in Latin "*quaranti giorni*") before sailors and guests could come on land. Quarantine is often thought of as a policy that separates individuals who may have been exposed to a contagious agent regardless of symptoms. Isolation is, generally speaking, considered a severe form of quarantine, often put in place in response to high morbidity and mortality. Quarantine was used extensively in the treatment and control of tuberculosis in Europe first and later, at end of the nineteenth century, in the USA. The emergence of SARS in 2003 re-instated the world's interests in the concepts of Isolation and Quarantine (Q & I), the only initial methods available of disease control [11, 19].

The concepts of Q & I have multiple working meanings and uses. Hence, selecting a definition depends on the disease, the suspected level of risk that it poses to others, the means and modes of transmission, and the system's knowledge and experience with the infectious agent. Regardless of the definition used, one of the challenges associated with Q & I strategies is that there is hardly any reliable assessments of their population level efficacy. There are no effective

quantitative frameworks that account for direct and indirect economic losses and/or the costs associated with the implementation of Q & I strategies (but see [14, 27–29, 33, 34, 38, 40]).

Critical to any method of assessment comes from the fact that dynamic models that include the Q & I classes disease must be prepared to account for their sometimes destabilizing impact on the disease dynamics (sustained oscillations). The introduction of Q & I classes can generate the kind of dynamics where assessing the effectiveness of interventions may be difficult. Feng et al. showed in [24, 25], for example, that the incorporation of a quarantine or isolation class (Q) was enough to destabilize the unique disease endemic equilibrium in a susceptible–infected–recovered (SIR) model. These results were confirmed by Hethcote and collaborators [31] using alternative SIQR modeling frameworks.

Tracing exposed individuals, assuming that a test exists that determines if an individual is infected or not, and their contacts, would make it possible to quarantine or isolate diagnosed infectives, a first step towards assessing the impact of Q & I [15]. Models are used to address questions like: What impact will placing a fixed proportion of individuals living in the "neighborhood" of an index case in quarantine have on disease control? We observe that when large numbers are involved, the costs and challenges become immense. Should isolated individuals be kept at their homes or moved to designated quarantine facilities?

In [39] a two-strain influenza model is studied to investigate competitive outcomes (mediated by cross-immunity) that result from the interactions between two strains of influenza A in a population where sick individuals may be quarantined or isolated. The inclusion of a quarantined class makes the model analysis much more challenging due to the presence of sustained oscillations and possible other bifurcations. To make the analysis more transparent, an SIQR model with a single strain is presented first.

*9.7.1 *An SIQR Model with a Single Infectious Class*

In this section, results in [24] and [25] are revisited in order to highlight the impact of the inclusion of quarantine and/or isolation classes in generating sustained periodic solutions from SIQR epidemic models.

Let $S(t)$, $I(t)$, $Q(t)$, and $R(t)$ denote the susceptible, infective, quarantined, and recovered classes, respectively, and let $N = S+I+Q+R$ denote the total population size. Model parameters are: μ, the per-capita rates for birth and death; γ, the rate at which infected individuals are isolated (quarantined); δ, recovery rate; and β, the transmission rate. The SIQR model can be formulated as follows:

$$\begin{aligned}
\frac{dS}{dt} &= \mu N - \beta S\frac{I}{N-Q} - \mu S,\\
\frac{dI}{dt} &= \beta S\frac{I}{N-Q} - (\mu+\gamma)I,\\
\frac{dQ}{dt} &= \gamma I - (\mu+\delta)Q,\\
\frac{dR}{dt} &= \delta Q - \mu R
\end{aligned} \tag{9.27}$$

with appropriate initial conditions.

What makes the above model "distinct" is that the incidence rate now accounts for the possibility that a large number of individuals (those in the Q class) do not participate (by request, mandate, or personal decision) in the transmission process. Hence, the "random mixing" of infected proportion with other individuals is $\frac{I}{N-Q}$ rather than $\frac{I}{N}$.

The basic reproduction number for the above SIQR model is

$$\mathscr{R}_0 = \frac{\beta}{\mu+\gamma}. \tag{9.28}$$

It was shown in [25] that the disease-free equilibrium is globally asymptotically stable when $\mathscr{R}_0 < 1$. However, for $\mathscr{R}_0 > 1$, the behavior of model solutions is very different from the standard SIR model. That is, the unique endemic equilibrium, denoted by E^*, can become unstable due to the appearance of stable periodic solution via a Hopf bifurcation [32]. Notice from (9.28) that $\mathscr{R}_0$ is independent of the isolation period $1/\delta$. A bifurcation analysis using δ as the bifurcation parameter shows that E^* is asymptotically stable when the quarantine period is either very large or very small.

To facilitate the analysis, consider the following equivalent system with re-scaled parameters:

$$\begin{aligned}
\frac{dI}{d\tau} &= \left(1 - \frac{I+R}{N-Q}\right)I - (\nu+\theta)I,\\
\frac{dQ}{d\tau} &= \theta I - (\nu+\alpha)Q,\\
\frac{dR}{d\tau} &= \alpha Q - \nu R,
\end{aligned} \tag{9.29}$$

where $\tau = \beta t$ and

$$\nu = \frac{\mu}{\beta}, \quad \theta = \frac{\gamma}{\beta}, \quad \alpha = \frac{\delta}{\beta}.$$

The S equation has been eliminated as N is constant and $S = N - I - Q - R$. Note that the scaled parameter representing the isolation period is α. Based on the system (9.29), the following result on the possibility of periodic solutions via Hopf bifurcation was established in [25]:

Theorem 9.1 *There is a function, $\alpha_c(\nu)$, defined for small $\nu > 0$,*

$$\alpha_c(\nu) = \theta^2(1-\theta) + O(\nu^{1/2}),$$

such that there are two critical values α_{c1} and α_{c2} with the following properties:

(a) The endemic equilibrium is locally asymptotically stable if $1/\alpha < 1/\alpha_{c1}(\nu)$ or $1/\alpha > 1/\alpha_{c2}(\nu)$ and unstable if $1/\alpha_{c1}(\nu) < 1/\alpha < 1/\alpha_{c2}(\nu)$, as long as $1/\alpha$ is close to the critical values.

(b) Hopf bifurcations occur at $\alpha = \alpha_{ci}(\nu)$ $(i = 1, 2)$, leading to stable periodic solutions near the bifurcation points.

Further, at the bifurcation point corresponding to α_{c1}, the length of periods can be approximated by the formula

$$T \approx \frac{2\pi}{(1-\theta)^{1/2}\nu^{1/2}} \approx \frac{2\pi}{(\theta y^*)^{1/2}},$$

where $y^* = I^*/(N - Q^*)$ is the proportion of infectious individuals at the endemic equilibrium scaled by the active population, $N - Q$.

With parameter values relevant to scarlet fever, numerical simulations of the model confirm the occurrence of two Hopf bifurcation points, which are illustrated in Fig. 9.8. The right plot in Fig. 9.8 shows two Hopf bifurcation points (labeled by HB) occurring for values of the average quarantine periods in two distinct ranges near $1/\alpha_{ci}$ $(i = 1, 2)$. The plot on the left shows the enlarged portion near the lower bifurcation point $1/\alpha_{c1}$, with the curves labeled with SP representing the maximum and minimum of the stable periodic solutions. The solid and dashed curves labeled by SSS and USS represent stable steady state and unstable steady state (showing the I^* component of the endemic equilibrium E^*), respectively.

It was pointed out in [24, 25] that only the region near the lower critical point $1/\alpha_{c1}$ is relevant for childhood diseases, and that the data on the length of reported isolation periods during the 1897–1978 scarlet fever epidemics in England and Wales [2] were very close to the range that supports periodic solutions for model (9.29) near $1/\alpha_{c1}$.

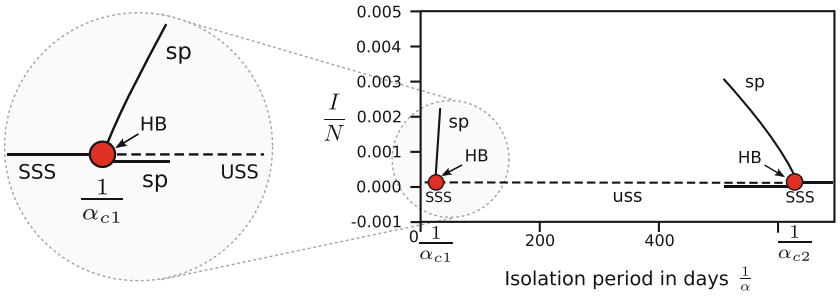

Fig. 9.8 The plot on the right is a bifurcation diagram based on numerical simulations of the system (9.29) with parameter values relevant to scarlet fever. The solid and dashed curves (labeled by SSS and USS) represent the fraction of the I components when the endemic equilibrium E^* is stable and unstable, respectively, depending on the value of the isolation period $1/\alpha$. The right plot shows two Hopf bifurcation points, α_{c1} and α_{c2}, labeled by HB. An enlarged version of the right HB is shown on the left. The solid curves labeled with sp illustrate the maximum and minimum of the stable periodic solutions

Several extensions of the model (9.27) have been considered including [23, 31, 49]. For example, the model in [23] reads

$$\begin{aligned}
\frac{dS}{dt} &= \mu N - \beta S\frac{I}{N-\sigma Q} - \hat{\beta} S\frac{(1-\sigma)Q}{N-\sigma Q} - \mu S,\\
\frac{dI}{dt} &= \beta S\frac{I}{N-\sigma Q} + \hat{\beta} S\frac{(1-\sigma)Q}{N-\sigma Q} - (\gamma+\kappa+\mu)I,\\
\frac{dQ}{dt} &= \gamma I - (\delta+\mu)Q,\\
\frac{dR}{dt} &= \kappa I + \delta Q - \mu R.
\end{aligned} \tag{9.30}$$

In (9.30), individuals in the I class can recover without going through the Q class. In addition, the degree of effectiveness (i.e., reducing the movement of quarantined individuals) is considered through the use of the parameter σ with $\sigma = 1$ and 0 corresponding to a perfect and ineffective quarantine/isolation, respectively. It is shown in [23] that the likelihood for the existence of sustained oscillations depends on σ.

Because Hopf bifurcations are local properties, and because the bifurcation diagram generated by numerical simulations in Fig. 9.8 seems to suggest that the periods of the periodic solutions for parameters away from the Hopf bifurcation points become very large, it indicates the possibility for a homoclinic bifurcation. This is explored in [51]. It was shown in [51] that a center manifold reduction of the system (9.27) at a bifurcation point has the normal form $x' = y$, $y' = axy + bx^2y + O(4)$, indicating a bifurcation of codimension greater than two. Here, x and y are variables after several changes of variables from the system (9.29). By considering an unfolding of the normal form, it was shown that a perturbed system can indeed generate a homoclinic bifurcation. This is illustrated in Fig. 9.9.

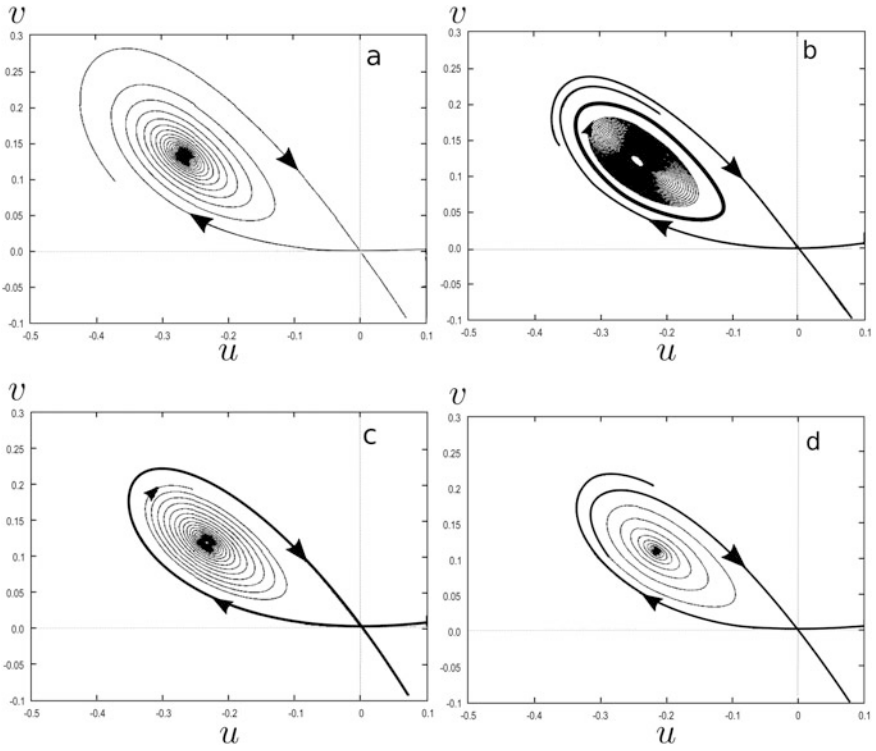

Fig. 9.9 Numerical simulations of a perturbed system of the normal form reduction from the system (9.29). The four plots correspond to four sets of parameter values near the homoclinic bifurcation. As the parameter values change, the interior equilibrium E^* changes from stable to unstable leading to the appearance of a stable periodic solution (see plots (**a**) and (**b**)), and that a homoclinic bifurcation occurs as parameter values change from (**b**) to (**d**), in which case, a homoclinic solution exists (see (**c**))

The four sub-figures a–d in Fig. 9.9 demonstrate trajectories of the perturbed system for four sets of parameter values. It shows first that the stability of E^* switches from stable to unstable with the appearance of a stable periodic solution (see a and b). As parameter values continue to change from b to c, the system undergoes a homoclinic bifurcation, in which case, the stable periodic solution expends its magnitude and eventually disappears after reaching the saddle point (see b–d) and a homoclinic orbit appears (see c).

*9.7.2 *The Case of Two Strains with Cross-Immunity*

The SIQR model (9.27) can be extended to include two pathogen strains. The description of the two-strain model requires the division of the population into ten different classes: susceptibles (S), infected with strain i (I_i, primary infection),

isolated with strain i (Q_i), recovered from strain i (R_i, as a result of primary infection), infected with strain i (V_i, secondary infection), given that the population had recovered from strains $j \neq i$, and recovered from both strains (W). The population is assumed to mix randomly, except that the mixing is impacted by the process of quarantine/isolation [15, 25, 31]. Using the flow diagram in Fig. 9.10, we arrive at the model

$$\begin{aligned}
\frac{dS}{dt} &= \Lambda - \sum_{i=1}^{2} \beta_i S \frac{(I_i + V_i)}{A} - \mu S, \\
\frac{dI_i}{dt} &= \beta_i S \frac{(I_i + V_i)}{A} - (\mu + \gamma_i + \delta_i) I_i, \\
\frac{dQ_i}{dt} &= \delta_i I_i - (\mu + \alpha_i) Q_i, \\
\frac{dR_i}{dt} &= \gamma_i I_i + \alpha_i Q_i - \beta_j \sigma_{ij} R_i \frac{(I_j + V_j)}{A} - \mu R_i, \qquad j \neq i \\
\frac{dV_i}{dt} &= \beta_i \sigma_{ij} R_j \frac{(I_i + V_i)}{A} - (\mu + \gamma_i) V_i, \qquad j \neq i, \quad i, j = 1, 2 \\
\frac{dW}{dt} &= \textstyle\sum_{i=1}^{2} \gamma_i V_i - \mu W, \\
A &= S + W + \textstyle\sum_{i=1}^{2} (I_i + V_i + R_i),
\end{aligned} \tag{9.31}$$

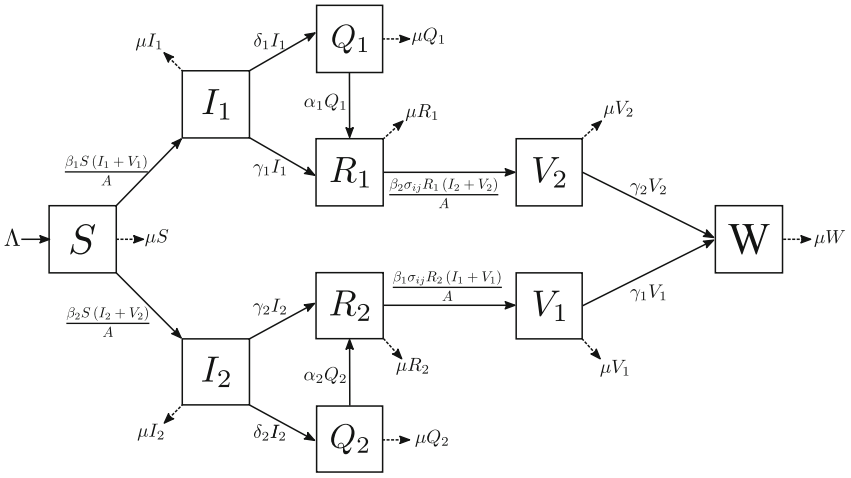

Fig. 9.10 Schematic diagram of the dynamics in host exposed to two co-circulating influenza strains. Λ is the rate at which individuals are born into the population, β_i denotes the transmission coefficient for strain i, μ is the per-capita mortality rate, δ_i is the per-capita isolation rate for strain i, γ_i denotes the per-capita recovery rate from strain i, α_i is the per-capita rate at which individuals leave the isolated class as a result of infection with strain i, and σ_{ij} is the relative susceptibility to strain j for an individual that has been infected with and recovered from strain i ($i \neq j$). $\sigma_{ij} = 0$ corresponds to total cross-immunity, while $\sigma_{ij} = 1$ indicates no cross-immunity between strains. The protection is said to be strong if $0 \leq \sigma_{ij} \ll 1$, and weak if $0 \ll \sigma_{ij} \leq 1$

where A denotes the population of non-isolated individuals and $\frac{\beta_i S(I_i+V_i)}{A}$ models the rate at which susceptibles become infected with strain i. That is, the ith $(i \neq j)$ incidence rate is assumed to be proportional to both the number of susceptibles and the available modified proportion of i-infectious individuals, $\frac{(I_i+V_i)}{A}$. The parameter σ_{ij} is a measure of the cross-immunity provided by a prior infection with strain i to exposure with strain j $(i \neq j)$. It is assumed that $\sigma_{ij} \in [0, 1]$. Model (1) includes the models in [13, 16]. The omission of the Q classes in earlier work precludes the possibility of sustained oscillations (see [13, 16]) in the absence of population (age) structure.

System (9.31) has at least four equilibria. Analysis of the local stability of the trivial equilibrium (absence of disease) helps identify conditions under which the "flu" can invade. Hence, we first focus on establishing the conditions that make it impossible (at least locally) for both strains to invade a disease-free population, simultaneously. In the analytical results obtained here it is assumed that $\sigma_{12} = \sigma_{21} = \sigma$.

The basic reproduction number for the two strains is

$$\mathscr{R}_i = \frac{\beta_i}{\mu + \gamma_i + \delta_i}.$$

Using the perturbation technique based on the fact that μ is a much smaller parameter than other parameters, we can identify two curves in the $(\mathscr{R}_1, \mathscr{R}_2)$ plane that determine the stability of the non-trivial equilibria. Let $f(\mathscr{R}_1)$ and $g(\mathscr{R}_2)$ be two functions defined by

$$f(\mathscr{R}_1) = \frac{\mathscr{R}_1}{1 + \sigma(\mathscr{R}_1 - 1)\left(1 + \frac{\delta_2}{\mu+\gamma_2}\right)\left(1 - \frac{\mu(\mu+\alpha_1)}{(\mu+\gamma_1)(\mu+\alpha_1)+\alpha_1\delta_1}\right)} \tag{9.32}$$

and

$$g(\mathscr{R}_2) = \frac{\mathscr{R}_2}{1 + \sigma(\mathscr{R}_2 - 1)\left(1 + \frac{\delta_1}{\mu+\gamma_1}\right)\left(1 - \frac{\mu(\mu+\alpha_2)}{(\mu+\gamma_2)(\mu+\alpha_1)+\alpha_2\delta_2}\right)}. \tag{9.33}$$

Let $\mathscr{R}_i^* = \mathscr{R}_i$ $(i = 1, 2)$ evaluated at $\mu = 0$. Then the following result holds.

Theorem 9.2 *There exists a function $\alpha_{1c}(\mu)$ defined for small $\mu > 0$ by*

$$\alpha_{1c}(\mu) = \frac{\delta_1}{\mathscr{R}_1^*}(1 - \frac{1}{\mathscr{R}_1^*}) + O(\mu^{1/2}),$$

with the following properties: (i) The boundary endemic equilibrium E_1 is locally asymptotically stable if $\mathscr{R}_2 < f(\mathscr{R}_1)$ and $\alpha_1 < \alpha_{1c}(\mu)$, and unstable if $\mathscr{R}_2 > f(\mathscr{R}_1)$ or $\alpha_1 > \alpha_{1c}(\mu)$. (ii) When $\mathscr{R}_2 < f(\mathscr{R}_1)$, periodic solutions arise at $\alpha_1 = \alpha_{1c}(\mu)$ via Hopf bifurcation for small enough $\mu > 0$. The period can be approximated by

$$T = \frac{2\pi}{|\Im\omega_{2,3}|} \approx \frac{2\pi}{\left((\gamma_1+\delta_1)(\mathscr{R}_1^*-1)\right)^{\frac{1}{2}}\mu^{1/2}}.$$

Because we have focused on the symmetric case, an analogous result for the second boundary equilibrium E_2 can be stated immediately. That is, the boundary endemic equilibrium E_2 is locally asymptotically stable if $\mathscr{R}_1 < g(\mathscr{R}_2)$ and $\alpha_2 < \alpha_{2c}(\mu)$. It becomes unstable if $\mathscr{R}_1 > g(\mathscr{R}_2)$ or $\alpha_2 > \alpha_{2c}(\mu)$. A summary of the stability results as presented in Theorem 9.2 for strain 1 is obtained for strain 2 by replacing the parameter indices 1's with 2's and replacing $f(\mathscr{R}_1)$ with $g(\mathscr{R}_2)$. Functions $f(\mathscr{R}_1)$ and $g(\mathscr{R}_2)$ help determine the stability and coexistence regions for strains 1 and 2. In fact, changes in the regions of stability for a single and both strains can be illustrated by varying the coefficient of cross-immunity. For instance, from (9.32) we can compute the value of σ at which

$$f'(\mathscr{R}_1) \equiv \frac{\partial f(\mathscr{R}_1,\sigma)}{\partial \mathscr{R}_1}\Big|_{\sigma_1^*} = 0, \tag{9.34}$$

namely

$$\sigma_1^* = \frac{1}{\left(1+\frac{\delta_2}{\mu+\gamma_2}\right)\left(1-\frac{\mu(\mu+\alpha_1)}{(\mu+\gamma_1)(\mu+\alpha_1)+\alpha_1\delta_1}\right)}.$$

Hence, for all $\mathscr{R}_1 > 1$,

$$f'(\mathscr{R}_1) > (<\text{ or }=)\,0, \qquad f(\mathscr{R}_1) > (<\text{ or }=)\,1 \qquad \text{if } \sigma < (>\text{ or }=)\,\sigma_1^*.$$

These properties can be easily checked by noticing from (9.32) that

$$f(\mathscr{R}_1) = \frac{\mathscr{R}_1}{1+\frac{\sigma}{\sigma_1^*}(\mathscr{R}_1-1)} \quad \text{and} \quad f'(\mathscr{R}_1) = \frac{1-\frac{\sigma}{\sigma_1^*}}{\left(1+\frac{\sigma}{\sigma_1^*}(\mathscr{R}_1-1)\right)^2}.$$

Using the symmetry between two strains, we can show that similar properties hold for another threshold value σ_2^* (interchanging the subscripts 1 and 2 in the expression of σ_1^*) and a function $\mathscr{R}_1 = g(\mathscr{R}_2)$. The properties of f and g are illustrated in Fig. 9.11. The first two plots in Fig. 9.11 are for the special case when the two strains have identical parameter values ($\sigma_1^* = \sigma_2^* = \sigma^*$), whereas the last two plots are for the case $\sigma_1^* \neq \sigma_2^*$. $\mathscr{R}_2 < f(\mathscr{R}_1)$ is a necessary condition for the stability of strain 1 (either a stable boundary endemic equilibrium E_1 or the equilibrium associated with strain 1 oscillations). Hence, E_2 is unstable when $\mathscr{R}_2 > f(\mathscr{R}_1)$. Similarly, E_1 is unstable when $\mathscr{R}_1 > g(\mathscr{R}_2)$. Hence, coexistence is expected when $\mathscr{R}_2 > f(\mathscr{R}_1)$ and $\mathscr{R}_1 > g(\mathscr{R}_2)$.

Figure 9.12 depicts the stability of the equilibria and periodic solutions when $(\mathscr{R}_1, \mathscr{R}_2)$ lies in Regions I and III. It illustrates how the stabilities of equilibria and

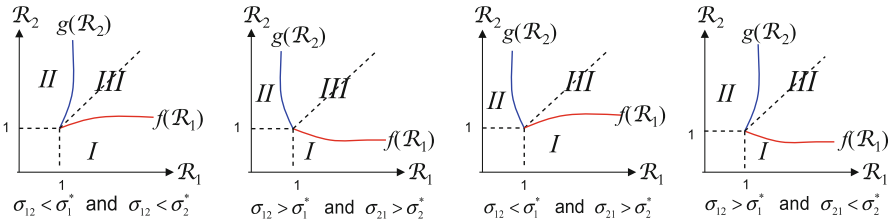

Fig. 9.11 Bifurcation diagrams in the $(\mathcal{R}_1, \mathcal{R}_2)$ plane for various combination of σ_1 and σ_2 values in relation to the threshold levels of σ_1^* and σ_2^* (cross-immunity). Regions I–III denote the existence and stability of E_1, E_2, and coexistence, respectively

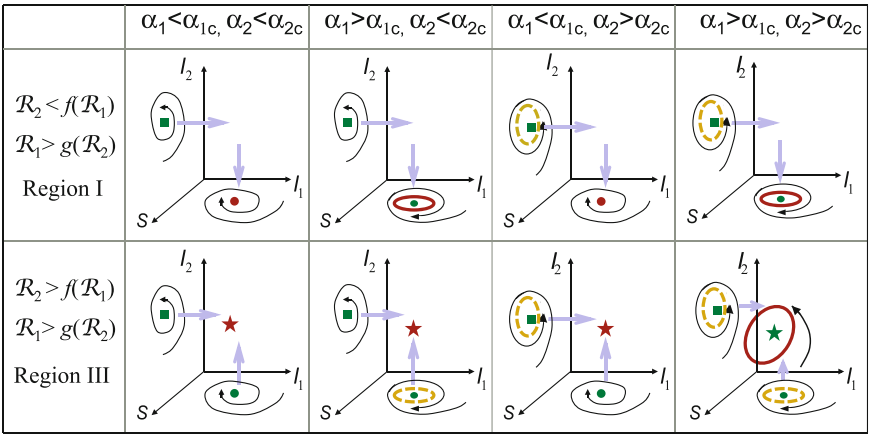

Fig. 9.12 Depiction of the stability properties of equilibria and periodic solutions for parameter values in different regions. A solid circle represents a stable boundary (strain 1 only) equilibrium. A solid square represents an unstable boundary (strain 2 only) equilibrium. A star represents a stable interior (coexistence of both strains) equilibrium. A solid (dashed) closed orbit represents a stable (unstable) period solution

periodic orbits change their stability when the parameters α_1 and α_2 change their values crossing the critical points α_{ic} $(i = 1, 2)$.

The focus of this study is on the time evolution of influenza A in a non-fixed landscape driven by tight coevolutionary interactions (that is, interactions where the fate of the host and the parasite are intimately connected) between human hosts and competing strains. The process is mediated by intervention (behavioral changes) and cross-immunity. In other words, the nature of the invading landscape (susceptible host) changes dynamically from behavioral changes (isolation, short time scale) and past immunological experience (cross-immunity, long time scale).

The "partial" herd immunity generated by past history of invasions on the host population can have a huge impact on the quantitative dynamics of the "flu" at the population level. The assumption that $\sigma_{12} = \sigma_{21} = \sigma$ for $i \neq j$ naturally results in a dynamic landscape that is not too different (in the oscillatory regime) than

the one observed on single-strain models with isolation [25, 31]. That is, a lack of heterogeneity in cross-immunity results in a system "more or less" driven (in the oscillatory regime) by the process of isolation.

The results show that multiple strain coexistence is highly likely for antigenically distinct (weak cross-immunity) strains and not for antigenically similar under symmetric cross-immunity ("competitive exclusion" principle [10]) . As the levels of cross-immunity weaken, the likelihood of sub-threshold coexistence increases. However, "full" understanding of the evolutionary implications that result from human host and influenza virus interactions may require the study of systems that incorporate additional mechanisms such as seasonality in transmission rates, age structure, individual differences in susceptibility or infectiousness, and the possibility of coinfections. Thacker [46] notes that the observed seasonality of influenza in temperate zones may be the key to observed patterns of recurrent epidemics. Superinfection may also be a mechanism worth consideration, even though studies in [46] show that it is only moderately possible for young individuals to become infected with two different strains in one "flu" season.

9.8 Exercises

1. Write the basic influenza model of Sect. 9.2 as an age of infection model and calculate its basic reproduction number.
2. Write the vaccination model of Sect. 9.2.1 as an age of infection model and calculate its reproduction number. [Warning: In order to do this, you will need to formulate a heterogeneous mixing age of infection model because vaccinated and unvaccinated individuals have different infectivities and susceptibilities.]

In the analysis of seasonal and pandemic influenza in this chapter, we have used simple SIR models. However, influenza has a more complicated structure, with exposed periods and asymptomatics. The obvious way to include this more complicated structure would be to use age of infection models.

3. Formulate an age of infection model analogous to the seasonal epidemic model (9.13), and calculate its reproduction number and final size relation.
4. Formulate an age of infection model analogous to the pandemic influenza model (9.18), and calculate its reproduction number and final size relation.
5. Formulate an age of infection model analogous to the combined seasonal/pandemic influenza model (9.21) and calculate its reproduction number.
6. Consider the model (9.14) in Sect. 9.4. Choose parameters to make the basic reproduction number equal to 1.5, take $\sigma_i = 1 - q^i$, where $q = 0.75$, and $\tau_i = 1$. Simulate the model and determine the final sizes.
7. Use the final sizes obtained from Exercise 6 as initial sizes and repeat the simulation. Repeat this several times to see if the final sizes approach limits.

8. Use the limiting final sizes obtained in Exercise 7 as initial sizes and simulate the model (9.18) of Sect. 9.5 with parameters giving a basic reproduction number of 2. Determine the final size of the pandemic.
9. Simulate the model (9.21) of Sect. 9.5 for various values of ρ between 0 and 1. For which values do seasonal and pandemic strains coexist and for which values does the pandemic strain replace the seasonal strain? (References: [3, 4, 8].)

References

1. Alexander, M.E., C.S. Bowman, Z. Feng, M. Gardam, S.M. Moghadas, G. Röst, J. Wu & P. Yan (2007) Emergence of drug resistance: implications for antiviral control of pandemic influenza, Proc. Roy. Soc. B **274**: 1675–1684.
2. Anderson, G. W., R.N. Arnstein, and M.R. Lester (1962) Communicable Disease Control, Macmillan, New York.
3. Andreasen, V. (2003) Dynamics of annual influenza A epidemics with immuno-selection, J. Math. Biol. **46**: 504–536.
4. Andreasen, V., J. Lin, & S.A. Levin (1997) The dynamics of cocirculating influenza strains conferring partial cross-immunity, J. Math. Biol. **35**: 825–842.
5. Arino, J., C.S. Bowman &S.M. Moghadas (2009) Antiviral resistance during pandemic influenza: implications for stockpiling and drug use, BMC Infectious Diseases **9**: 1–12.
6. Arino, J., F. Brauer, P. van den Driessche, J. Watmough & J. Wu (2006) Simple models for containment of a pandemic, J. Roy. Soc. Interface **3**: 453–457.
7. Arino, J., F. Brauer, P. van den Driessche, J. Watmough & J. Wu (2008) A model for influenza with vaccination and antiviral treatment, Theor. Pop. Biol. **253**: 118–130.
8. Asaduzzaman, S.M., J. Ma, & P. van den Driessche (2015) The coexistence or replacement of two subtypes of influenza, Math. Biosc., **270**:1–9.
9. Bootsma, M.C.J. & N.M. Ferguson (2007) The effect of public health measures on the 1918 influenza pandemic in U.S. cities, Proc. Nat. Acad. Sci. **104**: 7588–7593.
10. Bremermann, H. J. and H.R. Thieme (1989) A competitive exclusion principle for pathogen virulence, J. Math. Biol. **27**:179–190.
11. Brown, D. (2003) A Model of Epidemic Control, The Washington Post, Saturday, May 3, 2003; Page A 07. http://www.washingtonpost.com/ac2/.
12. Brauer, F., P. van den Driessche, & J. Watmough (2010) Seasonal and pandemic influenza: Strategic and tactical models, Can. Appl. Math. Q. **19**: 139–150.
13. Castillo-Chavez, C (1987) Cross-immunity in the dynamics of homogenous and heterogeneous populations, **87** (37), Mathematical Sciences Institute, Cornell University.
14. Castillo-Chavez, C. and G. Chowell (2011) Special Issue: Mathematical Models, Challenges, and Lessons Learned from the 2009 A/H1N1 Influenza Pandemic, Math. Biosc. Eng. **8**(1): 246 pages, (http://aimsciences.org/journals/displayPapers1.jsp?pubID=411)
15. Castillo-Chavez, C., C. Castillo-Garsow, and A.A. Yakubu (2003) Mathematical models of isolation and quarantine. JAMA, **290**: 2876–2877.
16. Castillo-Chavez, C., H.W. Hethcote, V. Andreasen, S.A. Levin, and W.M. Liu (1989) Epidemiological models with age structure, proportionate mixing, and cross-immunity, J. Math. Biol. **27**: 233–258.
17. CDC (2011) Weekly Influenza Surveillance Report 2009-2010 Influenza Season, http://www.cdc.gov/flu/weekly/weeklyarchives2009-2010/weekly20.htm.
18. Conway, J.M., A.R.Tuite, D.N. Fisman, N. Hupert, R. Meza, B. Davoudi, K. English, P. van den Driessche, F. Brauer, J. Ma, L.A. Meyers, M. Smieja, A. Greer, D.M. Skowronski, D.L. Buckeridge, J. Kwong, J. Wu, S.M. Moghadas, D. Coombs, R.C. Brunham, & B. Pourbohloul

(2011) Vaccination against 2009 pandemic H1N1 in a population dynamic model of Vancouver, Canada: timing is everything, Biomed Central Public Health **11**: 932.
19. Chowell, G., P.W. Fenimore, M.A. Castillo-Garsow, and C. Castillo-Chavez (2003) SARS Outbreaks in Ontario, Hong Kong and Singapore: the role of diagnosis and isolation as a control mechanism, J. Theor. Biol. **24**(1): 1–8.
20. Chowell, G., C.E. Ammon, N.W. Hengartner, & J.M. Hyman (2006) Transmission dynamics of the great influenza pandemic of 1918 in Geneva, Switzerland: Assessing the effects of hypothetical interventions, J. Theor. Biol. **241**: 193–204.
21. Chowell, G., C.E. Ammon, N.W. Hengartner, & J.M. Hyman (2007) Estimating the reproduction number from the initial phase of the Spanish flu pandemic waves in Geneva, Switzerland, Math. Biosc. & Eng. **4**: 457–479.
22. Elveback, L.R., J.P. Fox, E. Ackerman, A. Langworthy, M. Boyd & L. Gatewood (1976) An influenza simulation model for immunization studies, Am. J. Epidem. **103**: 152–165.
23. Erdem, M., M. Safan, and C. Castillo-Chavez (2017) Mathematical analysis of an SIQR influenza model with imperfect quarantine, Bull. Math. Biol, **79**: 1612–1636.
24. Feng, Z. (1994) Multi-annual outbreaks of childhood diseases revisited the impact of isolation, Ph.D. Thesis, Arizona State University.
25. Feng, Z. and H.R.Thieme (1995) Recurrent outbreaks of childhood diseases revisited: the impact of isolation, Math. Biosc. **128**: 93–130.
26. Gardam, M., D. Liang, S.M. Moghadas, J. Wu, Q. Zeng & H. Zhu (2007) The impact of prophylaxis of healthcare workers on influenza pandemic burden, J. Roy. Soc. Interface, **4**: 727–734.
27. Fenichel, E.P., C. Castillo-Chavez, M.G. Ceddia, G. Chowell, P.A Gonzalez Parra, G.J. Hickling, G. Holloway, R. Horan, B. Morin, C. Perrings, M. Springborn, L. Velazquez, and C. Villalobos (2011) Adaptive human behavior in epidemiological models, Proc. Nat. Acad. Sci. **108**: 6306–6311.
28. Gonzalez-Parra, P., S. Lee, C. Castillo-Chavez, and L. Velazquez (2011) A note on the use of optimal control on a discrete time model of influenza dynamics, Math. Biosc. Eng. **8**: 193–205.
29. Gonzalez-Parra, P. A., L. Velazquez, M.C. Villalobos, and C. Castillo-Chavez (2010) Optimal control applied to a discrete influenza model. Conference Proceedings Book of the XXXVI International Operation Research Applied to Health Services, Book ISBN 13: 9788856825954 edited by Franco Angeli Edition.
30. Hannoun, C., F. Megas, and J. Piercy (2004) Immunogenicity and protective efficacy of influenza vaccination, Virus Research **103**: 133–138.
31. Hethcote, H.W., Z. Ma, and S. Liao (2002) Effects of quarantine in six endemic models for infectious diseases, Math. Biosc., **180**: 141–160.
32. Hopf, E. (1942) Abzweigung einer periodischen Lösungen von einer stationaren Lösung eines Differentialsystems, Berlin Math-Phys. Sachsiche Akademie der Wissenschaften, Leipzig, **94**: 1–22.
33. Lee, S., G. Chowell, and C. Castillo-Chavez (2010) Optimal control of influenza pandemics: The role of antiviral treatment and isolation, J. Theor. Biol. **265**: 136–150.
34. Lee, S., R. Morales, and C. Castillo-Chavez (2011) A note on the use of influenza vaccination strategies when supply is limited, Math. Biosc. Eng. **8**: 179–191.
35. Longini, I.M., M.E. Halloran, A. Nizam, & Y. Yang (2004) Containing pandemic influenza with antiviral agents, Am. J. Epidem. **159**: 623–633.
36. Lipsitch, M., T. Cohen, M. Murray & B.R. Levin (2007) Antiviral resistance and the control of pandemic influenza PLoS Med. **4**: e15.
37. Manuel, O., M Pascual, K. Hoschler, S. Giulieri, K. Ellefsen, P. Bart, J. Venetz, T. Calandra, and M. Cavassini (2011) Humoral response to the influenza A H1N1/09 monovalent AS03-adjuvanted vaccine in immunocompromised patients, Clinical Infectious Diseases **52**: 248–256.
38. Mubayi, A., C. Kribs-Zaleta, M. Martcheva, and C. Castillo-Chavez (2010) A cost-based comparison of quarantine strategies for new emerging diseases, Math. Biosc. Eng. **7**: 687–717.

39. Nuno, M., Z. Feng, M. Martcheva, and C. Castillo-Chavez (2005) Dynamics of two-strain influenza with isolation and partial cross-immunity, SIAM J. Appl. Math. **65**: 964–982.
40. Prosper, O., O. Saucedo, D. Thompson, G. Torres-Garcia, X. Wang, and C. Castillo-Chavez (2011) Control strategies for concurrent epidemics of seasonal and H1N1 influenza, Math. Biosc. Eng. **8**: 147–177.
41. Public Health Agency of Canada, Vaccine Development Process, URL http://www.phac-aspc.gc.ca/influenza/pandemic-eng.php.
42. Qiu, Z. & Z. Feng (2010) Transmission dynamics of an influenza model with vaccination and antiviral treatment, Bull. Math. Biol. **72**: 1–33.
43. Stillianakis, N.I., A.S. Perelson & F.G. Hayden (1998) Emergence of drug resistance during an influenza epidemic: insights from a mathematical model, J. Inf. Diseases, **177**: 863–873.
44. Olinsky, R., A. Huppert & L. Stone (2008) Seasonal dynamics and threshold governing recurrent epidemics, J. Math. Biol. **5**6: 827–839.
45. Stone, L., R. Olinsky & A. Huppert (2007) Seasonal dynamics of recurrent epidemics, Nature **446**: 533–536.
46. Thacker, S. B. (1986) The persistence of influenza A in human populations, Epidemiologic Reviews, **8**: 129–142.
47. Towers, S., and Z. Feng (2009) Pandemic H1N1 influenza: Predicting the course of pandemic and assessing the efficacy of the planned vaccination programme in the United States, Eurosurveillance, **14**(41): Article 2.
48. van den Driessche, P. & J. Watmough (2002) Reproduction numbers and subthreshold endemic equilibria for compartmental models of disease transmission, Math. Biosc. **180**:29–48.
49. Vivas-Barber, A., C. Castillo-Chavez, and E. Barany (2014) Dynamics of an "SAIQR" influenza model, Biomath, **3**: 1–13.
50. Welliver, R., A.S. Monto, O. Carewicz, E. Schatteman, M. Hassman J. Hedrick, H.C. Jackson, L. Huson, P. Ward & J.S. Oxford (2001) Effectiveness of oseltamivir in preventing influenza in household contacts: a randomized controlled trial, JAMA **285**: 748–754.
51. Wu, L. and Z. Feng (2000) Homoclinic bifurcation in an SIQR model for childhood disease, J. Differential Equations, **168**: 150–167.